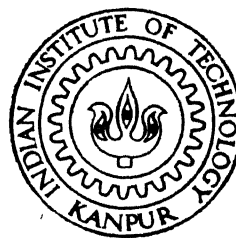


A SCHEME OF ADAPTIVE TURNING OPERATION

by

ESWAR KUMAR KUNISETTY



DEPARTMENT OF MECHANICAL ENGINEERING

INDIAN INSTITUTE OF TECHNOLOGY KANPUR

JUNE, 1997

ME
1997
M
KVN
SCH

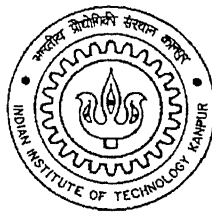
A SCHEME OF ADAPTIVE TURNING OPERATION

A Thesis Submitted
in Partial Fulfillment of the Requirements
for the Degree of

MASTER OF TECHNOLOGY

by

ESWAR KUMAR KUNISSETTY



to the

**DEPARTMENT OF MECHANICAL ENGINEERING
INDIAN INSTITUTE OF TECHNOLOGY
KANPUR**

June, 1997

- 8 JUL 1997

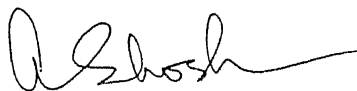
CENTRAL LIBRARY
U. S. T., KANPUR

Vol. No. A 123580

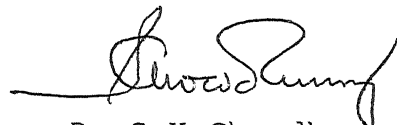
ME-1997 - M - KUN - SCH

CERTIFICATE

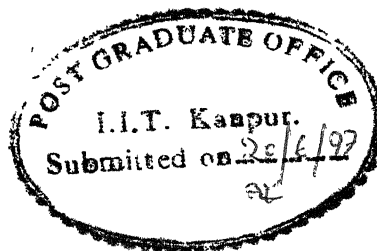
It is certified that the work contained in the thesis entitled " A SCHEME OF ADAPTIVE TURNING OPERATION " by ESWAR KUMAR KUNISETTY, has been carried out under our supervision and this work has not been submitted elsewhere for a degree.



Dr. Amitabha Ghosh,
Professor,
Dept. of Mech. Engineering,
IIT KANPUR.



Dr. S.K. Choudhary,
Associate Professor,
Dept. of Mech. Engineering,
IIT KANPUR.



Dedicated

to

MY BELOVED PARENTS

ACKNOWLEDGEMENTS

I express my sincere thanks to my thesis supervisors Dr.Amitabha Ghosh and Dr.S.K.Choudhury for their support and guidance rendered during my stay here at I.I.T. Kanpur. Their constant encouragement has been vital factor in the development of the present work. Their active support and the discussions made my first endeavour in research more enjoyable.

I am thankful to all the students of the Manufacturing Science stream for maintaining the tempo and lively atmosphere with discussions. Special thanks to Rao, Rammohan, Rama Rao, Ranganatha, Manas De, Siva, Ragni, Seshagiri, Ramprasad, Yugandhar and Santosh.

Many thanks to Mr.R.M.Jha, Mr.Bajaj, Mr.Namdeo, Mr.H.P.Sharma, Mr.Prem Prakash and Mr.Deepak. Their experience and expertise has been of immense help in solving many of the practical problems encountered.

Finally I express thanks to my friends Pandu, Sivasree, Seshu, Giridhar, Ghanta, Shanti, Rajgopal, Ramesh and Bhole who made my stay here a memorable and eventful one.

Abstract

The objective of the present work is to evaluate optimal cutting conditions using minimum experimentation. A tool-life model based on the assumption that adhesive wear is the predominant wear mechanism has been developed. In the present work only flank face wear has been considered which is prevalent at low and moderate cutting speeds. The growth of the flank wear has been sensed in terms of increase in the normal force. Analysis has been carried out for steel workpieces and HSS, carbide tools. Gilbert's model of economics of cutting has been used for evaluating optimal cutting conditions. Based on the tool-life model, an Adaptive Control System (*ACS*) has been developed for on-line tool wear monitoring. The results obtained using the model have been compared with the experimental results.

Contents

1	AUTOMATED MANUFACTURING	1
1.1	Tool Wear and Tool Life	3
1.2	Probable Causes of Tool Failure	5
1.3	Adaptive Control	7
1.4	Motivation For The Present Work	8
1.5	Organization of the Thesis	9
2	THEORETICAL ANALYSIS	10
2.1	Methods of Determining Tool-Life Data	12
2.2	On-Line Tool Wear Sensing	13
2.3	Tool Wear Models	14
2.4	Tool Life and Optimal Cutting Conditions	18
2.5	Effect of Tool Wear on Cutting Forces	20
3	MATHEMATICAL MODELLING of TOOL WEAR	22
3.1	Mathematical Modelling	22
3.2	Flank Wear Model	23
4	EXPERIMENTATION	32
4.1	Experimental Setup	32
4.2	Instrumentation	34

4.2.1	Transducer	34
4.2.2	Amplifier	36
4.3	Analog to Digital Conversion	38
4.4	Experimental Procedure	41
5	RESULTS and DISCUSSION	43
5.1	Machining of Steel with HSS	43
5.2	Validation of the Model	44
5.3	Discussion	49
6	CONCLUDING REMARKS	50
6.1	Scope for future work	50
	REFERENCES	52
	APPENDIX	55

List of Figures

1.1	Different types of tool wear	4
1.2	Growth of flank wear with time	5
1.3	Adaptive control system	7
2.1	Variation of tool life with speed	12
2.2	economics of cutting	19
3.1	Variation of hardness for various tool materials with temperature . .	25
3.2	Variation of Diffusion Co-efficient with temperature	25
3.1	Variation of Temperature with Cutting speed [24]	26
3.2	Tool Geometry (Flank wear volume)	27
3.3	Relationship between flank wear and cutting force system on worn tool	28
3.4	Plot between Normal Force and h_f	29
3.5	Increase in Normal force with Wear land and at different cutting speeds	31
4.1	Schematic diagram of the experimental setup	33
4.2	Photograph showing the experimental setup	33
4.3	Dynamometer	35
4.4	Tool holder	36
4.5	Strain gauges	36
4.6	Amplification circuit	37
4.7	Successive approximation ADC , [26]	39

4.8	Flowchart for analog-to-digital conversion	40
4.9	Algorithm for the Application program	42
5.1	Variation of diffusion coefficient of carbon with respect to 0.3% C steel	44
5.2	Variation of normal force with time at cutting speed, $56m/min$. . .	46
5.3	Variation of normal force with time at cutting speed, $72m/min$. . .	47
5.4	Variation of normal force with flank wear land	47
5.5	Variation of flank wear land with time	48
5.6	Cutting speed V vs Tool life	49

List of Tables

2.1	Typical tool wear sensing methods and sensors for cutting force . . .	21
3.1	Relationship between normal load and wear rate	23
5.1	Experimental values at $56m/min$	45
5.2	Experimental values at $72m/min$	45

Nomenclature

A	=	The rate of increase of normal load with respect to increase in wear at the flank, kg/mm.
b	=	width of cut, mm.
D	=	diffusion coefficient.
h_f	=	wear-land at the principal flank surface, mm.
h_f^*	=	critical value of wear-land, mm.
H	=	hardness, kg/sq mm.
m	=	index depending upon the deformation type at contact zone.
n	=	Taylor's exponent on tool-life.
p	=	index of cutting velocity in tool-life equation.
R	=	universal gas constant.
T	=	time, min.
U	=	activation energy.
V_c	=	Cutting velocity, mm/min.
Z	=	wear coefficient.
α	=	index giving the slope of the diffusion curve.
α_o	=	clearance angle, deg.
γ_o	=	rake angle, deg.
θ_f	=	flank temperature, deg K absolute.
$\bar{\theta}_f$	=	flank temperature, deg C.
V_{opt}	=	optimum cutting speed.
t_{ct}	=	tool change time.
λ_1	=	cost/min of labour and overheads.
λ_4	=	total cost of each regrinding of tool.

Chapter 1

AUTOMATED MANUFACTURING

The objective of the present work is to evaluate optimal cutting conditions with minimum experiments. To determine optimal conditions tool-life equation should be well defined. In the present work tool-life is determined by correlating the increase in the cutting force to tool wear

Advances in modern technology in manufacturing sciences have produced great strides in our ability to accomplish efficiently the production of goods through automated systems to the extent that computers now directly control machining operations.

Development of fully automated machine tools, unmanned machining centers, efficient flexible manufacturing systems and adaptive control optimization of the machining process have been and would continue to be the subject of interest and research for manufacturing engineers. Efficiency, quality and productivity are the key considerations in these systems. Minimizing human intervention during the manufacturing processes, without any loss of reliability and thus reducing the risk of human errors have been an operational strategy in realizing these systems.

Current research on fully automated production includes complete computer control from design through inspection and packaging. And yet, although the seemingly straightforward task of precisely predicting the useful tool life has been examined by scores of researchers for almost three-quarters of a century, it still remains an extremely difficult and troublesome problem. This kind of computer control for tool wear must be very precise if economically optimized production is to be maintained in today's sophisticated, automated manufacturing systems.

Versatile automation can, in fact, be achieved to some degree at any one of the following three different levels of control:

- 1 Feedback control.
- 2 Supervisory control.
3. Self-optimising control.

Feedback control is the oldest and least versatile of these three levels of control since it can accept only a limited number of inputs. Supervisory control, such as numerical control machining operation, is more versatile since it can be continuously change operating conditions such as feeds and speeds at the command of constantly changing inputs supplied by a program. However, supervisory control is pre-programmed and will thus achieve optimality only if the assumptions upon which the program is based do not change. Self-optimising control, such as the adaptive control of a machine tool, does not suffer from this limitation since it is self-adjusting in that it continually determines and sets the optimal working conditions on the basis of in-process measurements of the appropriate parameters.

1.1 Tool Wear and Tool Life

The tool-life which has been defined as the usable time that has elapsed before the cutting tool has failed can be expressed in terms of the causes affecting failure of cutting tools.

The cutting tool may fail due to lack of transverse strength when the force acting on the tool increases beyond the permissible limit. Hence cutting force can be used as an indication for evaluation of tool-life. Similarly cutting speed which causes thermal softening resulting in "form stability" of the cutting tools can also be used as an indication for evaluation of tool life.

However the most commonly used criterion for the evaluation of tool-life is the amount of wear that has taken place in the rake or flank surfaces of the cutting tool. Hence often the tool-life investigations centered around the manner and magnitude of the wear process of the cutting tool. Therefore, a thorough analysis of wear mechanism including their role in the failure process of the cutting tool is of considerable interest and importance in metal cutting technology.

The various types of wear a cutting tool may be subjected to are illustrated in Fig. 1.1. Of these, flank wear on the nose and the primary cutting edge (FW) with its accompanying notch (N) and crater wear on the rake face (CW) are classified as regular types wear. They are always present in a machining operation and have "regular" cutting time related growth characteristics. Because of these reasons, flank wear and crater wear have generally formed the subject of the most studies in the area of tool wear. The other types of tool wear are generally avoided by proper selection of tool material and cutting conditions. Because of these reasons and their irregular, unpredictable nature when they occur, irregular wear phenomenon, such as breakage, etc., have not been considered in this work.

The variables affecting tool life may be listed as:

1. The cutting conditions - speed, feed and depth of cut.

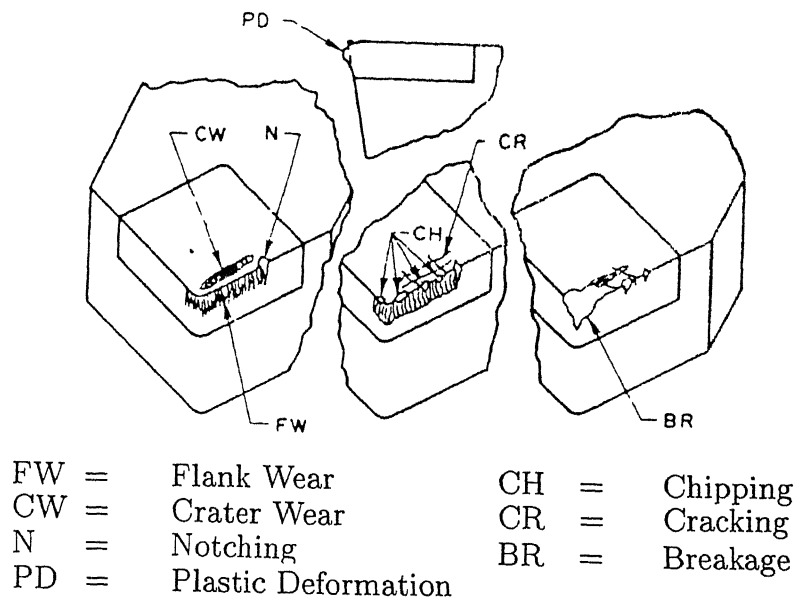


Figure 1.1: Different types of tool wear

2. The tool geometry.
3. The tool material.
4. The work material.
5. The cutting fluid.

In addition, the type and condition of the machine tools used are also important.

The growth of the wear land with respect to time is shown in Fig 1.2. Up to point Q, the region denotes the zone of initial break-in. The sharp edge rapidly breaks due to plastic deformation and consequential temperature rise. After that the wear process is more or less uniform until the point F is reached. This region is the gradual mechanical (linear) wear, and constitutes the major part of the tool life. Beyond the point F, the rapid growth of wear process ensues and the cutting tool fails very soon after reaching this point of inflexion F, called the critical flank wear point. The point of inflexion F depends on the critical temperature.

The different processes by which the failure of cutting tool may occur are:

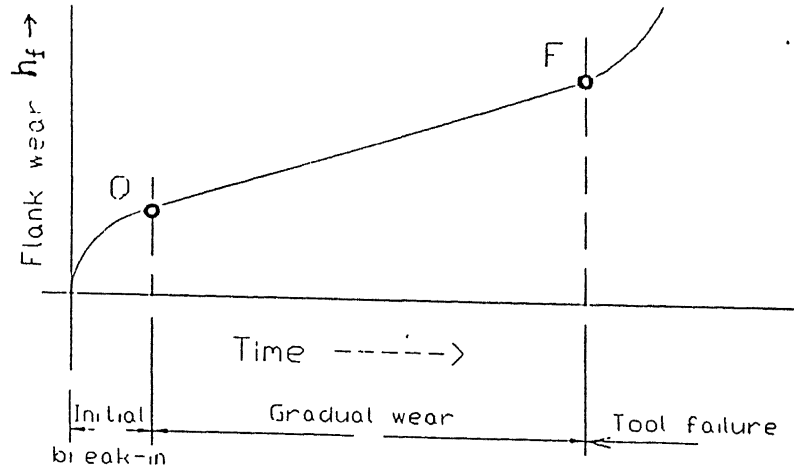


Figure 1.2: Growth of flank wear with time

- Failure by brittle fracture due to lack of transverse strength of the basic wedge constituting the cutting tool.
- Rise in interface temperature through increase of feed and cutting speed may cause failure through loss of form stability.
- Even if the tool has sufficient strength against brittle fracture as well as against plastic deformation, the cutting tool still fails by the process of wear which is defined as gradual loss of tool material through mutual interaction between the chip and tool material and work and tool material.

1.2 Probable Causes of Tool Failure

Wear which can be described as the total loss of weight of the sliding pairs accompanying friction, is classified in four basic classes.

Abrasion wear : It is due to ploughing by hard constituents including the fragments of the built-up-edge as they are swept over the tool surface.

Adhesion wear : When the metallic surfaces are brought into intimate contact under moderate loads, a metallic bond between adjoining materials takes place.

This phenomenon is known as "Adhesion". When the pressure between the contact surfaces is very high and the pairs are in continuous relative motion, the nascent surface layers of the machined job and the chip strong bonding between the two parts are formed along the real area of contact, the adhesive spots. As the stress at any given spot varies in the cyclic fashion due to the relative motion of the surfaces, the dripping off of that particular spot from its mother body is connected with fatigue phenomenon. A model of transfer of metal under such conditions has been developed by Archard [1] considering the removal in lumps. But when the pressure is extremely high and the area of contact is very small, a uniform contact between the surfaces may exist. For this case the model of layer removal instead of lump removal will be more appropriate. Quantity of metal transfer is apparently proportional to the area of contact, as well as to the hardness ratio of the mating pair under prevalent environment.

Diffusion Wear : If the mechanical process involved in the adhesion is capable of increasing the localized temperature of the real area of contact of a surface, interfacial diffusion will occur allowing a more intimate approach of the two surfaces. Wear at higher cutting speeds is often attributed to the process of diffusion.

Chemical wear : It is due to the interaction between the mating surfaces, in the presence of a fluid. If the fluid is active to the tool, wear rate may be accelerated by chemical reaction. In cutting operation with cutting fluids, the chemical wear process may influence the tool-wear phenomenon and tool life.

Electrolytic wear : Electrolytic wear is the wear process which is due to possible galvanic corrosion between tool and work piece materials.

1.3 Adaptive Control

The study and monitoring of the progression of tool wear during the cutting operation and its effect on the outcome of the operation is paramount to incorporating an adaptive control systems in the machine tool.

The need for today's complex manufacturing systems and wage structure requires the use of machine tools operated by means of an adaptive controlled system. Adaptive control provides a continuous monitoring of performance and adjusts the system variables in order to approach the optimum conditions for chosen performance objectives.

There are basically three functions which determine an adaptive controlled system (Fig. 1.3)

- Identification
- Decision
- Modification

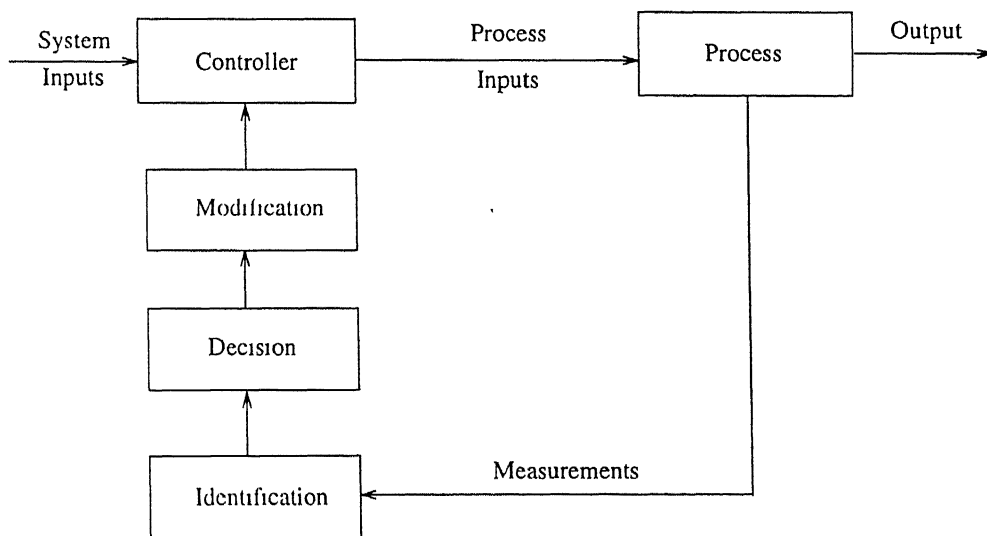


Figure 1.3: Adaptive control system

The identification measures the actual state of the process performance without taking its quality into consideration. In the second function, the received information is the basis for calculation comparing the actual state of performance with a desired one. The decisions can be directed toward minimum or maximum process conditions or any required values between these extreme points. The modification function is the corrective action needed to adaptively control the process.

The identification function which measures the actual performance relies mainly on sensing devices to monitor some of the process variables such as cutting forces, power consumption, tool deflection, tool wear, and so on.

1.4 Motivation For The Present Work

Advanced automation demands evaluation of optimal cutting conditions in minimum time. Accurate determination of cutting conditions is also essential. Understanding of the variations in material properties with cutting temperature is essential for developing accurate tool life models. Recent works were based on statistical methods, requiring large amount of data; in other words, large number of experiments and are computationally expensive. Hence there has been a need for a model which can evaluate optimal conditions in minimum time with less amount of data. An Adaptive control system is essential for on-line tool wear monitoring in an industry. The present work is an attempt to fulfill these needs.

In the present work a theoretical model which can evaluate Taylorian exponent ' n ' and constant ' C ' using minimum number of experiments (one experiment) has been developed. The model will be the basis for an Adaptive Control System (*ACS*) for on-line tool wear monitoring. The cutting conditions, various costs involved in manufacturing and h_f^* are inputs for the *ACS* and optimum cutting conditions (for minimum cost or for maximum production rate) should be the output.

1.5 Organization of the Thesis

The organization of the thesis is as follows:

Chapter 2 discusses about theoretical analysis, the various models of tool wear - tool life in turning.

Chapter 3 discusses in detail of proposed modifications to the model developed by Ghosh, and implementation of the proposed model.

Chapter 4 discusses the experimental setup instrumentation, and cutting conditions.

Chapter 5 discusses in depth about the validation of the model and the experimental results.

Chapter 6 concludes with the scope of future work.

Chapter 2

THEORETICAL ANALYSIS

Of the regular types of tool wear, only flank wear and the resulting recession of the cutting edge directly affects workpiece dimension and workpiece quality. Thus the single most significant type of wear that has drawn constant attention is flank wear. Ways and means of predicting it or measuring it has been the pursuit of researchers of several decades.

The most fundamental approach to this problem of tool wear has been to define a critical amount of flank wear-land. When this amount of wear is reached during machining, it is assumed that the tool has reached the end of its useful life. Since the rate of development of flank wear is a function of material and cutting process variables, F.W.Taylor first proposed the relationship as:

$$VT^n = C \quad (2.1)$$

where,

T	=	tool life
V	=	cutting speed
C, n	=	are constants depending on tool and work material, tool geometry, and cutting conditions (except speed).

The derivation of the Taylor tool-life equation enables the factors affecting the tool-life constant C [2] to be enumerated viz., C will increase, i.e., tool life will improve for a given tool material work-piece material combination

- as the value of the flank wear land criterion increases,
- as the clearance, rake angles increase,
- as the uncut chip thickness, uncut chip width decrease,
- as the cutting edge radius decreases, i.e., as the cutting edge becomes sharper,
- as the lubrication becomes more efficient,
- as the tool hardness increases and as the ductility of the material decrease,
- as the tool material thermal conductivity increases,
- as the workpiece hardness decreases, and
- as the thermal diffusivity of the workpiece material increases.

Fig. 2.1 [3] shows the typical variation of tool life with speed for *HSS*, *WC*, and ceramic tools, keeping the other conditions same. It is clear that the tool life for a given speed is normally much higher with *WC* than that with *HSS*. A ceramic tool performs better at a high cutting speed.

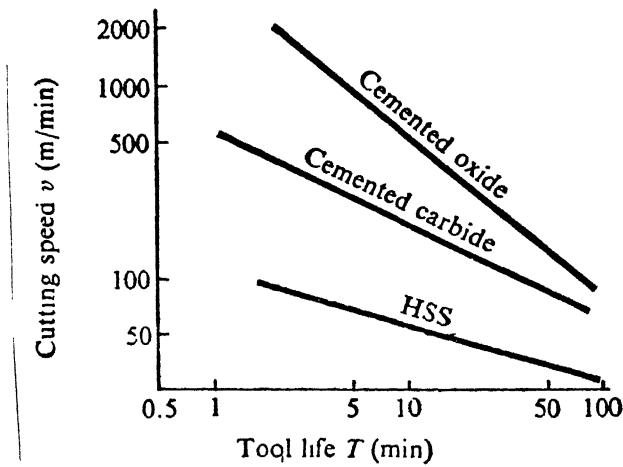


Figure 2.1: Variation of tool life with speed

Work material: AISI 1045; hardness, 170 BHN;
 tool geometry, -10, -10, 10, 10, 15, 15, 1.5mm;
 uncut thickness, 0.25mm; width of cut, 1.6mm;
 tool life based on 0.4mm flank wear.

2.1 Methods of Determining Tool-Life Data

The determination of tool-life data and tool-life equations has presented considerable difficulties. Tool-life testing is dependent on tool wear, and like most wear test, is both expensive and time-consuming to perform. The number of variables to be considered is large, to say the least; the tool geometry and material, the work material, the cutting conditions, the tool-failure criterion and other variables have to be included in tool-life determinations. The problem is nevertheless one which must be solved if economical cutting conditions are to be achieved.

Tool-life tests may be of the conventional type, which require large machining

time, or quick tool-life tests which require lesser machining time. Various approximate methods are also used to save costs and labour. In practical circumstances the variables are somewhat reduced, since the work material is normally known and tool material, geometry and cutting fluid, can be tentatively selected from handbooks, manuals and manufactures catalogues or recommendations. The number of variables considered will usually depend on how thorough an investigation is warranted.

Armarego [4] gives details of some of the approximate methods. In one method the cutting conditions are selected to give long tool-life values, the tool-wear is measured past the initial rapid wear stage and decision is made regarding the wear rate. In another method, the tool is run to a wear land w_1 for a cutting time T_1 and the time to reach the wear-land failure size is found by proportions, i.e.,

$$T = \frac{w_f}{w_1} T_1 \quad (2.2)$$

where w_f is wear land criterion.

This method ignores the initial rapid wear stage and is not as accurate as the conventional and quick tool-life methods. The same author [4] gives quick tool-life testing technique. The quick tool-life testing technique involves using cutting conditions, usually the cutting speed, which give short tool-life values of the order of a few minutes. These tests can be run in a way similar to the conventional tests, although this method is often associated with facing tests. Taper turning method has been suggested as an alternative method.

2.2 On-Line Tool Wear Sensing

The techniques for on-line tool wear sensing are divided in two main categories [5]: (a) direct tool wear sensing and (b) indirect tool wear sensing. Direct tool wear sensing, which implies that the actual progress of the physical wear on the

tool while cutting is being sensed on line, includes such methods as : radioactive; pneumatic; electrical resistance; optical; and other sensing techniques.

Indirect tool wear sensing relies on monitoring other variables in the process. These other variables are fairly correlated to the progression of wear and are presumably easier to sense. Methods for indirect tool wear monitoring include the change in: cutting forces and/or their ratios; workpiece dimensions; surface finish; cutting temperature and vibration.

2.3 Tool Wear Models

Davies [6] suggested Monte-Carlo model for mechanical wear process based on a few hypothesis which are

1. the quanta of energy are added to the rubbing particles all of which having same size;
2. the quanta of energy are added to the particles at domains randomly spaced over the surface and at moments randomly spaced in time;
3. the quantized energy added to the particle over surface diffuses continuously into the material at a known rate;
4. sufficient energy of a particle causes it to detach itself as a wear particle.

Considering the contact deformation of the high points of the asperities where point-to-point contact occurs, the energy generated due to contact deformation first appears at the surface and then gradually diffuses into the material following an exponential decay. Davies calculated and compared the wear particle size distribution to test the validity of the model by Monte-Carlo method for deriving the residual energy.

Dawil [7] reported that mutual diffusion of materials at a particular ‘adhesion temperature’ causing welding of certain constituents is the main reason of adhesion and transfer of type of wear.

Trent [8] forwarded that a fused layer of alloy is formed between steel and free WC of the tool. Wear was thought to be the consequence of carrying of the fused alloy by the moving chip.

Theoretical analysis of the adhesion phenomenon at the rake surface by Loladze [9] shows that the amount of material transferred from one surface to the other is a rather complex function. For a given tool-work pair, he deduced an expression for the distance traversed by the cutting tool before getting dull in the following form

$$V T = \text{constant} \left(\frac{H_1}{H_2} \right)^z \quad (2.3)$$

V = cutting speed,

T = duration of cut,

where H_1 = hardness of the contact layers of tool during cutting,

H_2 = hardness of contact films during cutting,

z = a constant depending on material pair.

From the above equation it follows that, for a constant tool life, the rate of cutting speed is proportional to the ‘contact hardness ratio (H_1/H_2)’.

Ghosh [10] deduced a theoretical model for wear growth under conditions of predominant adhesion, which has been the basis for the present work. This model has been modified to suit our objective, the details of which have been dealt with in the next chapter.

DeVore *et.al.*, [11] investigated into the nature of the variation of tool life over a range of cutting conditions for a finish turning process. They discussed the tool life variation and its influence on the development on tool life models. To account for the variation, the method of weighted least squares is employed in developing

a tool-life predicting equations. A comparison between the weighted least-squares method and the ordinary (unweighted least-squares method) is presented. More realistic predicting capabilities resulted by using the weighted method given the inherent behaviour of the tool life variations.

Realizing from the literature on metal turning the strong interrelationship between a changing force spectrum and tool wear, a theoretical model was presented by Akgerman ^{et.al.} [12] which relates the wear on flank and rake faces of tool tip to the cutting force vectors and the changing depth of cut on work piece. These essential linear relationships have been experimentally verified. The theoretical model was developed in two sections. The first section deals with the expected geometry caused by wear considering the lost rake face area and decrease in uncut chip cross-section. The second section deals with observed variations in cutting force, F_c and their relationship to both the decrease in uncut chip cross sectional area and increase in flank wear land.

A stochastic tool life model taking into account the main causes of failure was developed by Roseetto *et.al.*, [13]. A tool life model based on the assumption that wear and fracture are the causes of tool failure is re-examined from the theoretical standpoint, and extended to include the effect of cutting speed on the fracture-induced failure rate. On the assumption that tool life is terminated by various failure modes, but that wear, represented statistically by increasing hazard function, and accidental breakage, equivalent to a constant hazard function are the two main causes, a single-edge tool can be thought of as composed to two independent parts. A stochastic multi-edge tool life model was also discussed.

Koren *et.al.*, [14] proposed a model-based approach to on-line tool wear and breakage detection. A model-based approach is considered important for machining under variable cutting conditions, and for use with adaptive control systems that automatically adjust feed rates. The basic approach has been developed, and

illustrated with a simple simulation model. The simulation results confirm the feasibility of the proposed model-based approach, and indicate the need for further research to obtain experimental confirmation. They felt that further research was desirable on process modelling, estimation algorithms, and on-line training of the model-based approach by using artificial intelligence methods.

S.B.Rao [15] developed a microcomputer-based technique for monitoring the flank wear on single-point tool engaged in a turning operation. The technique is based on the real-time computation of a Wear Index (WI). The WI is a measure of the resistance, at the tool tip-workpiece interface along the flank, to the force oscillations of the cantilever portion of the tool holder, during machining. Increasing flank wear results in an increasing area of contact between tool tip and workpiece. This translates to an increasing WI , proportional to flank wear-land width and independent of other cutting process variables. This WI , which can be computed on-line as a ratio of the measured dynamic force amplitude to the vibration amplitude, at the first natural frequency of the cantilever portion of the toolholder, forms the basis of the microcomputer system.

Danai *et.al.*, [16] proposed a dynamic state model of tool wear which is suitable as the basis for an on-line tool wear sensing system. The model states include flank wear and crater wear, and the state equations are developed from available relationships in the literature. This nonlinear state model gives qualitatively responsible results, and is linearized and analyzed about particular operating conditions. These linearized equations provide a model structure, which together with on-line parameter estimation techniques, could be used to develop an adaptive observer for tool wear estimation.

The mathematical model of the wear-time-cutting condition relationships was found to be more appropriate in estimating wear levels only within the region of constant wear rate. Random disturbances of the tool such as chipping and fracture,

along with time at which a tool fails catastrophically, are not detectable by using this approach. The force ratio(F_z/F_y) variation due only to the wear progress, and ultimate tool failure, has been isolated through the development of nonlinear discrete models. An approach has been proposed by Oraby [17] in which the tool failure detection is made using the variation of the force ratio(F_z/F_y).

A unique technique is developed by Kaye *et.al.*, [18] for on line prediction of tool flank wear in turning using the spindle speed change. A mathematical model is presented for the approach. The speed sensing element is an optical encoder mounted on the spindle shaft and interfaced to an *IBM* microcomputer employing custom designed electronics. The changes in spindle speed are compensated for lathe transmission ratio, electrical configuration of the lathe's motor, and the torque speed relationship of the machine.

2.4 Tool Life and Optimal Cutting Conditions

Since the industry is very closely linked to economics and the machining operations play a predominant role in manufacturing parts, it is not difficult to appreciate the importance of studying the economic implications of the machining operations. The two parameters generally of interest are (i) cost and (ii) production time (rate). Both these depend on the choice of cutting parameters. T Figure 2.2 shows the variation of the various components of the cost with speed for a given feed.

Sometimes, the rate of production is more important than the cost per piece. In fact, from the economic point of view, the best situation is when the profit is maximum. A large rate of production may result in a better return, and hence useful to investigate the conditions leading to the highest possible rate of production. W.W.Gilbert[19]has developed a model for evaluating tool life for (i) minimum cost

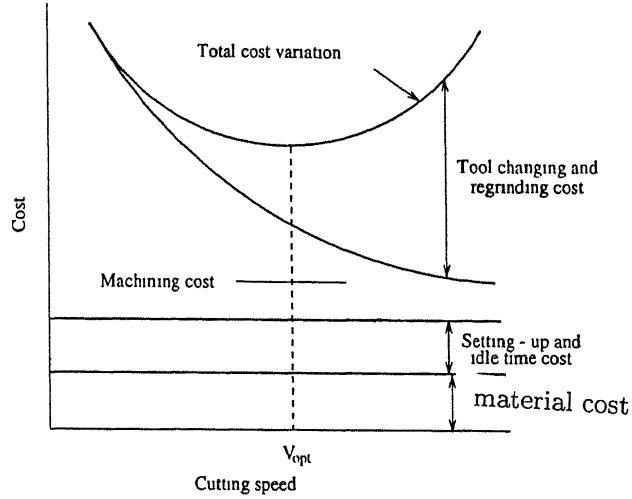


Figure 2.2: economics of cutting

and for (ii) maximum production rate. The optimum cutting speed for minimum cost(for a given value of feed) is given as

$$v_{opt} = \left[\frac{n C^{\frac{1}{n}} \lambda_1}{(1-n) (\lambda_1 tct + \lambda_4)} \right]^n \quad (2.4)$$

And the optimum cutting speed for maximum production rate is given by

$$v_{opt} = \left[\frac{n C^{\frac{1}{n}}}{(1-n) tct} \right]^n \quad (2.5)$$

where

v_{opt} = optimum cutting speed,

n = Taylor's tool life exponent,

C = constant in Taylor's tool life equation,

λ_1 = cost/min of labour and overheads,

λ_4 = total cost of each regrinding of the tool,

tct = is tool change time, min.

2.5 Effect of Tool Wear on Cutting Forces

One of the parameters that can be relatively easy to measure is cutting force. Cutting forces change as the tool wears out and have often been used to detect tool wear. Force sensing methods have been reported [20] to be more sensitive than vibration and power measurements. Some theoretical models based on force measurements have been presented in section 2.4.

The cutting force characteristics within the different phases of the tool working life have been investigated by Oraby [17] for a possible correlation with the various forms of tool failure. The effect of the different forms of tool wear and failure on the various force components is studied. Force-wear inter-relationships are formulated for possible use for in-process tool-state monitoring through measurement of the variation in cutting forces.

It has been investigated by Micheletti [21], Ghosh [10] that cutting forces increase almost linearly because of increase of normal force on the flank with growth of flank wear.

Most of the tool wear sensors in practical use are based on some kind of cutting force measurements. Typical sensing methods and sensors of the cutting force are summarized in Table 2.1 [22].

Table 2.1: Typical tool wear sensing methods and sensors for cutting force

Sensing method	Sensor	Remarks
Direct sensing		
Sensing by strain gauges (Octogonal ring, or diaphragm type sensor etc.)	Strain gauge	Dynamometer used mainly for research and development.
Sensing by combined strain gauge and acceleration pick-up	Strain gauge and ACC pick-up	
Sensing by piezo-electric force sensor	Piezo-electric transducer	
Sensing by load washer installed beneath the tool post or table	Strain gauge, Semi-conductor load transducer	Installed within machine tool.
Sensing by strain gauge attached to spindle	strain gauge	
Indirect sensing		
Estimation from deflection of spindle by proximeter pick-up	Eddy current type proximeter, Capacitive type proximeter	Installed within machine tool.
Estimation from deflection of tool post by electric micrometer	Differential transformer	
Estimation from power consumption of driving motor	Current meter, Watt meter	Simplified sensing.
Estimation from hydraulic pressure of hydro static bearing	Pressure transducer	
Estimation from slip rate of driving motor	Tacho-meter, Slip meter	

Chapter 3

MATHEMATICAL MODELLING of TOOL WEAR

3.1 Mathematical Modelling

From chapter 1 and 2 it is clear that the tool wear depends upon cutting conditions and material properties of both the tool and workpiece.

Machining process is basically plastic deformation process of work material through the application of force by cutting tool. The apparent strength (or resistance to plastic deformation) increases as the rate of deformation increases, whereas it becomes easier to deform a material at high temperature. Thus when speed of machining increases, the temperature of both the workpiece and tool increases, resulting in lowered effective hardness of tool material. Unfortunately the expected fall in hardness of work material is neutralized by high rate of deformation. Hence the variation in hardness of tool material with temperature was assumed as critical at the beginning of the investigation.

But on further analysis it was found that the variation of hardness is sensitive only above the critical point. Figure 3.1 shows the variation of hardness for various tool materials with temperature. For *HSS* tools below 538°C (critical

point) variation in hardness is moderate. Above critical point the hardness decreases exponentially.

Hence this idea has to be thrashed. On further investigation it was found that Ghosh's tool wear model[10] can be modified to suit our objective.

3.2 Flank Wear Model

Archard has shown that for different types of worn particles and depending on the nature of deformation which produces wear particles, the relationship between wear rate and applied load changes. The results obtained by Archard [1] are shown in the Table 3.1.

Table 3.1: Relationship between normal load and wear rate

Deformation	particle shape	Relationship between wear rate ($\frac{d\nu}{dt}$) and normal load (N)
Elastic	layer	$\frac{d\nu}{dt} \propto N^{3/5}$
	lump	$\frac{d\nu}{dt} \propto N^{4/5}$
Plastic	layer	$\frac{d\nu}{dt} \propto N^{3/4}$
	lump	$\frac{d\nu}{dt} \propto N$

The volumetric rate of wear can be expressed as

$$\frac{d\nu}{dt} = \frac{Z}{H} N^m V_c \quad (3.1)$$

where,

- H = hardness of softer of the tool-work pair,
- Z = wear coefficient depending upon materials in contact,
nature of contact and temperature of contact,
- N = normal load on surface,
- V_c = velocity of rubbing,
- m = exponent depending on nature of layer removed.

During metal cutting process the surfaces in contact are nascent and clean i.e., free from any contaminant layers. In this case it may be assumed that the wear rate will depend on the rate at which an interface material is formed through diffusion [10,23]. Therefore, the wear co-efficient Z will vary almost in the same manner as the diffusion co-efficient of tool material D , Z can be expressed as

$$Z = Z_o e^{-\frac{U}{R\theta_f}} \quad (3.2)$$

where,

- Z_o = a constant depending on the tool material,
- U = activation energy,
- R = universal gas constant,
- θ_f = absolute temperature at the flank, deg K.

It is also known that the diffusion co-efficient of a material (D) also varies in the same manner as Z , or,

$$D = D_o e^{-\frac{U}{R\theta_f}} \quad (3.3)$$

where D_o is a constant.

So from the variation of diffusion co-efficient of tool material variation of wear co-efficient can be predicted. Figure 3.2 shows variation of diffusion co-efficient with temperature (in general). The diffusion co-efficient in the working zone can be expressed as

$$D = D_o (\bar{\theta}_f)^p \quad (3.4)$$

where

$\bar{\theta}_f$ = flank temperature, deg C.,

$p = \tan \alpha$.

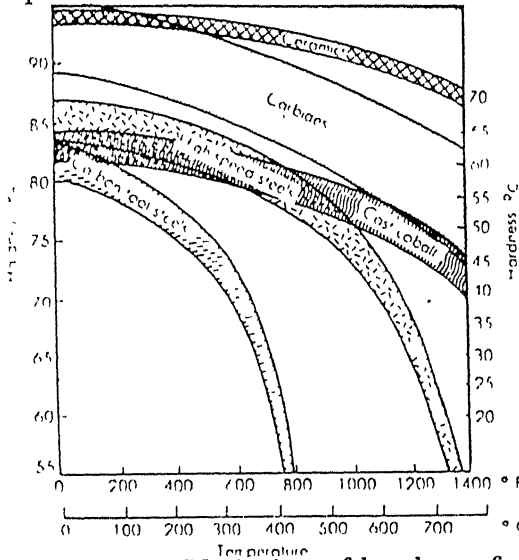


Figure 3.1: Variation of hardness for various tool materials with temperature [27]

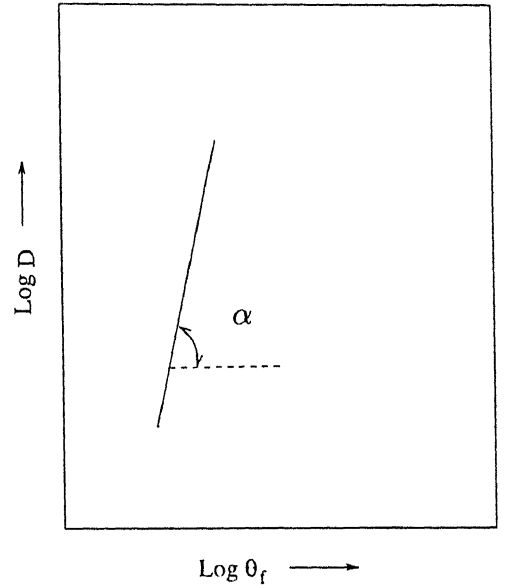


Figure 3.2: Variation of diffusion Co-efficient with temperature

Therefore it can be concluded that the wear co-efficient Z varies with flank temperature according to the following equation.

$$Z = Z_o (\bar{\theta}_f)^p \quad (3.5)$$

For the temperature insensitive region, average flank temperature, $(\bar{\theta}_f)_{avg}$ can be considered to be linearly dependent on $\sqrt{V_c}$ (Fig. 3.3). Hence the dependence of the average wear co-efficient \bar{Z} , in the temperature insensitive region (lower cutting speeds)

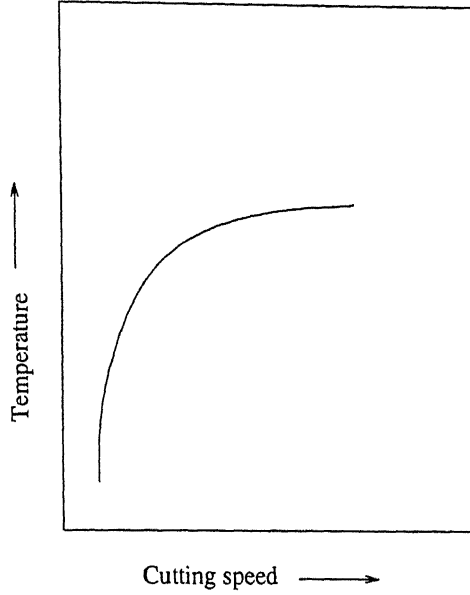


Figure3.3: Variation of Temperature with Cutting speed [24]

will be given by following equation

$$\bar{Z} = Z_o ([\bar{\theta}_f]_{avg})^p \quad (3.6)$$

where,

\bar{Z} = the average wear coefficient.

For the temperature insensitive region Eq. 3.6 can be written as

$$\bar{Z} = Z_o (\sqrt{V_c})^p \quad (3.7)$$

From the geometry of Fig. 3.4, the volume of worn tool material at any instant (t) during time interval (Δt) is ($d\nu$) given by

$$d\nu = b ds (h_f + \frac{dh_f}{2}) \quad (3.8)$$

where,

$$ds = \frac{dh_f \tan \alpha_o}{1 - \tan \alpha_o \tan \gamma_o} \quad (3.9)$$

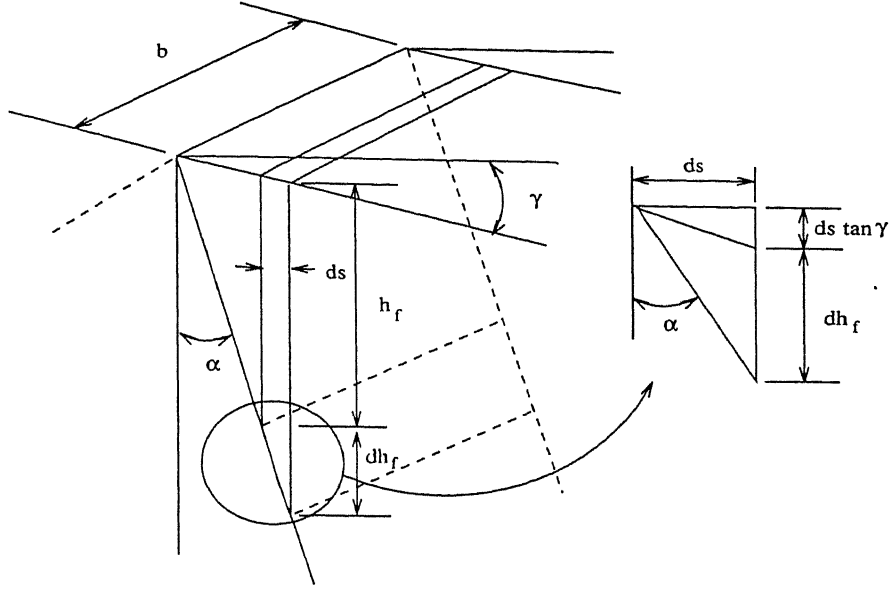


Figure 3.4: Tool Geometry (Flank wear volume)

Substituting Eq. 3.9 with Eq. 3.8 and neglecting terms of higher orders,

$$d\nu = \psi b h_f dh_f \quad (3.10)$$

The quantity ($\psi = \frac{\tan \alpha_o}{1 - \tan \alpha_o \tan \gamma_o}$) is dependent on tool geometry and can be assumed as a constant as long as a particular set of tool geometry is used.

Hence the rate of flank wear is,

$$\frac{d\nu}{dt} = b \psi h_f \frac{dh_f}{dt} \quad (3.11)$$

It is seen from Fig. 3.3 that the normal force N' at the flank wear land is dependent on the magnitude of h_f . It has been well established that in case of predominant flank wear and less intensive cratering, the normal force N' rises in direct proportion with h_f (Fig. 3.4).

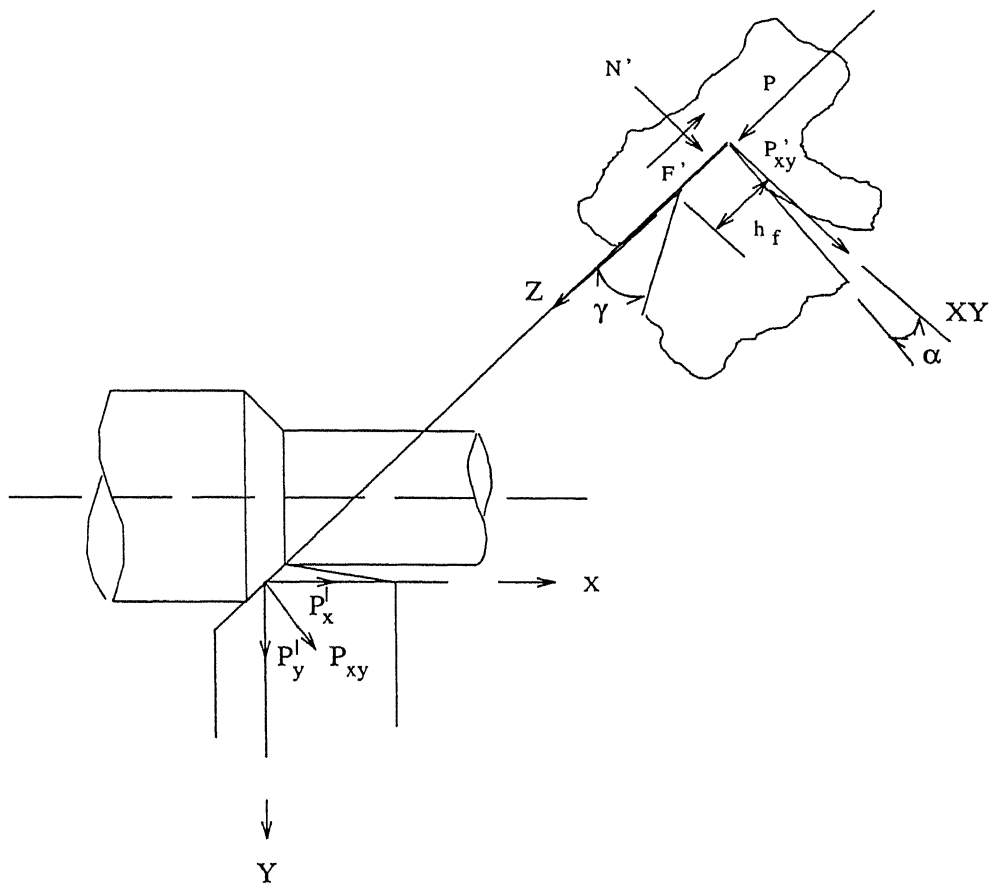


Figure 3.5: Relationship between flank wear and cutting force system on worn tool

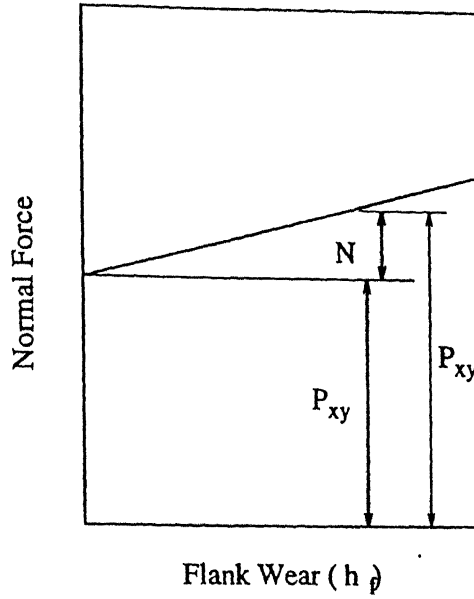


Figure 3.6: Plot between Normal Force and h_f

This relationship can be expressed in the form

$$N' = A h_f \quad (3.12)$$

where, $A = \frac{dN'}{dh_f}$ a constant for given cutting conditions and tool work material pair.

From equations (3.1), (3.7) and (3.12) the infinitesimal volume of wear can be written as

$$\begin{aligned} d\nu &= \left(\frac{Z_o}{H}\right) V_c^{\frac{\eta}{2}} N^m V_c dt \\ &= \left(\frac{Z_o}{H}\right) V_c^{(\frac{\eta}{2}+1)} N^m dt \end{aligned} \quad (3.13)$$

From equations (3.11) and (3.13)

$$b \psi h_f \frac{dh_f}{dt} = \left(\frac{Z_o}{H}\right) A^m h_f^m V_c^{(\frac{\eta}{2}+1)} \quad (3.14)$$

or,

$$h_f^{(1-m)} \frac{dh_f}{dt} = \left(\frac{Z_o}{H}\right) \frac{A^m V_c^{\frac{\eta}{2}+1}}{b \psi} \quad (3.15)$$

Integrating both the sides of the above equation with respect to time, t and putting the initial condition $h_f = 0$ at the $t = 0$, the above equation(Eq. 3.15) can be obtained in the form

$$\frac{1}{(2-m)} h_f^{(2-m)} = \left(\frac{Z_o}{H}\right) \frac{A^m V_c^{(\frac{p}{2}+1)} t}{b \psi} \quad (3.16)$$

or,

$$h_f = \left[(2-m) \left(\frac{Z_o}{H}\right) \frac{A^m}{b \psi} \right]^{\frac{1}{2-m}} V_c^{\frac{\frac{p}{2}+1}{(2-m)}} t^{\frac{1}{(2-m)}} \quad (3.17)$$

For temperature insensitive region, the wear process is by plastic layer removal, where $m = 3/4$ from Table. 3.1. Hence Eq. 3.17 may be written as

$$h_f = \left[\frac{5}{4} \left(\frac{Z_o}{H}\right) \frac{1}{b \psi} \right]^{0.8} A^{0.6} V_c^{(\frac{p}{2}+1)0.8} t^{0.8} \quad (3.18)$$

Eq. 3.18 can be written as

$$\left[\frac{h_f}{\left[\frac{5}{4} \left(\frac{Z_o}{H}\right) \frac{1}{b \psi} \right]^{0.8} A^{0.6}} \right]^{\frac{1}{(\frac{p}{2}+1)}} = V_c t^{\frac{1}{(\frac{p}{2}+1)}} \quad (3.19)$$

In the above equation, Z_o , a wear coefficient, is a constant for a given tool-work combination, and is available from the literature, b is width of cut, a constant for a particular cutting operation. H is the hardness of tool, can be assumed that there will not be significant variation in the working zone (below critical point). ψ depends on tool geometry and is a constant for a particular operation. A is the rate of increase of normal force with flank wear land. It has been found that A remains constant for a given cutting condition and tool-work material pair [25] (Fig. 3.7).

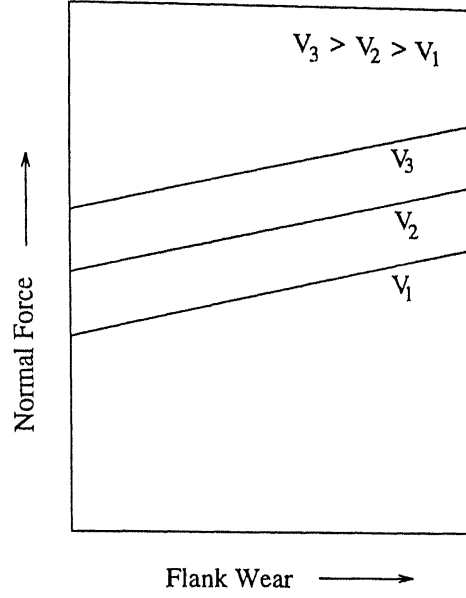


Figure 3.7: Increase in Normal force with Wear land and at different cutting speeds

Therefore for a given wear land criterion (h_f^*) Eq. 3.19 may be written as,

$$\left[\frac{h_f^*}{\left[\frac{5}{4} \left(\frac{Z_a}{H} \right) \frac{1}{b\psi} \right]^{0.8} A^{0.6}} \right]^{\frac{1}{(\frac{n}{2}+1)}} = V_c T^{\frac{1}{(\frac{n}{2}+1)}} \quad (3.20)$$

From the above explanation it is clear that Eq. 3.20 may be written as,

$$V_c T^n = C \quad (3.21)$$

which is nothing but Taylor's tool life equation.

Chapter 4

EXPERIMENTATION

To determine optimal cutting conditions tool-life equation should be well defined. In the present work tool-life is determined by correlating the increase in the cutting force to tool wear. The Taylor's tool-life exponent ' n ' and constant ' C ' along with cutting parameters and various manufacturing costs are the inputs to the software developed whose output is optimum cutting speed for a selected criterion.

4.1 Experimental Setup

A schematic diagram of the experimental setup is shown in Fig. 4.1. The forces coming on the cutting tool are sensed by the dynamometer. The dynamometer is calibrated before using for the force sensing. The tool overhang is maintained constant for all the experiments. The dynamometer output signal being in millivolts, the signal from the dynamometer is fed to an amplification circuit, the gain of which can be varied. The amplification gain is set to a certain level before starting the experiments. The amplifier and dynamometer are powered using a regulated *DC* power supply system of model No. *HIL* 3161. Figure 4.2 shows the photograph of the experimental setup.

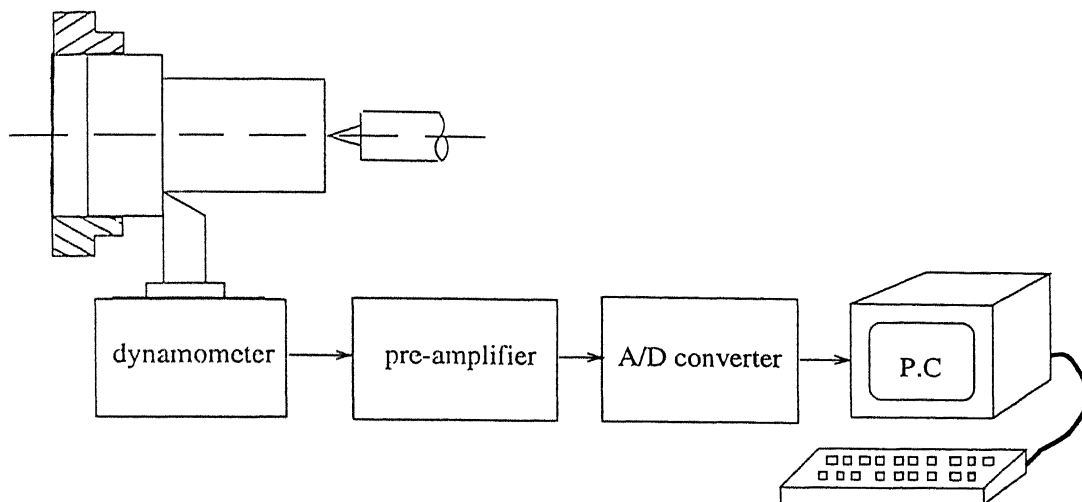


Figure 4.1: Schematic diagram of the experimental setup

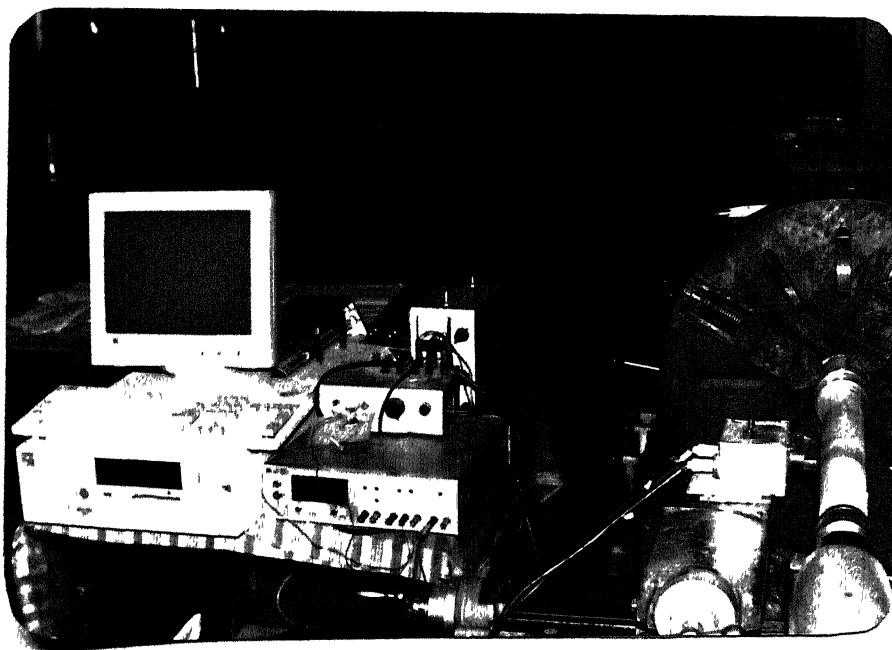


Figure 4.2: Photographing the experimental setup

the *IBMPC*. Initial switch settings are made on the analog-to-digital card for selecting the operating range. Using the software developed by the author a trigger is passed to the converter indicating the *START OF CONVERSION* and on receiving the *END OF CONVERSION* signal the converted data are transferred to a particular memory location. It is programmed to obtain the data after every 0.1sec.. After every 50 conversions, the average value of all the 50 readings is determined and taken as the sensor output signal(in digital form). As the tool wear phenomenon is known to be a gradual one, averaging of the values is done to take care of the small variations in the sensor output.

The cutting conditions (cutting speed, feed, depth of cut), tool geometry, various costs involved in manufacturing are the inputs to the program.

4.2 Instrumentation

4.2.1 Transducer

The measurement of cutting forces are performed either by measuring directly the deformation due to the cutting forces or by measuring the transformed deformation by a transducing element. The most widely used dynamometers employ transducing elements which convert mechanical deformations into electrical signals. Various forms of electrical devices used to convert mechanical deformations into electrical signals are (i) capacitive, (ii) piezo-electric, (iii) inductance, (iv) strain gauge pick-up.

A two component cutting force dynamometer of cantilever type is used in the present work. The design of the dynamometer is illustrated in Fig. 4.3. The dynamometer structure is made of aluminium. The action of the cutting force is to bend the structure. The vertical component of the resultant force (F_c) bends the structure about the axis A-A and the horizontal component (F_f) bends it

about axis B-B. Strain gauges were used to measure these distortions (moments), and the recordings are calibrated to give a measure of the forces applied. Bonded wire strain gauges with resistance 120 ohms, and gauge factor 2, have been used. Strain gauges were cemented with guaging wires parallel to the dynamometer axis O-O. The free end of the dynamometer structure accomadates a tool holder shown in the Fig. 4.4.

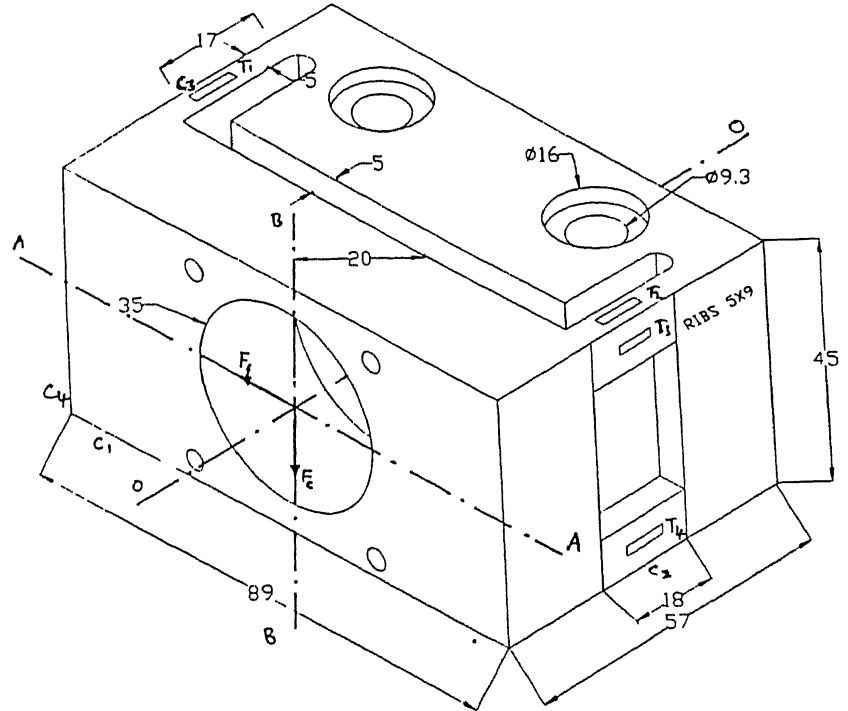


Figure 4.3: Dynamometer

To measure the moment M_c , due to force F_c , two strain gauges are cemented to the top of the measuring section (T_1 and T_2) and two gauges are cemented directly below (C_1 and C_2) thus, when M_c is applied, two gauges are put in tension, while two others receive an equal amount of compression, thereby satisfying the requirements for a complete Wheatstone bridge (Fig. 4.5a). In a similar manner moment M_f , due to force F_f , is measured by four gauges T_3, T_4, C_3, C_4 which are connected as shown in (Fig. 4.5b).

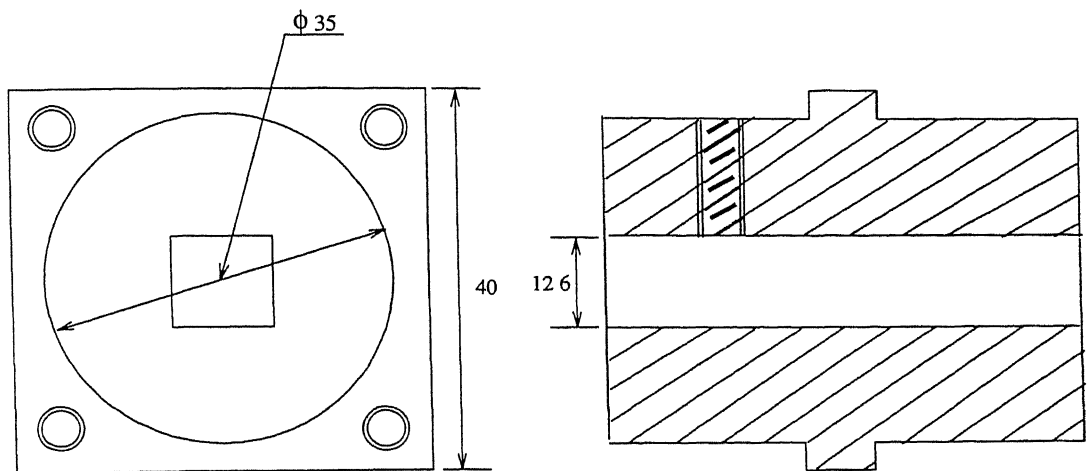


Figure 4.4. Tool holder

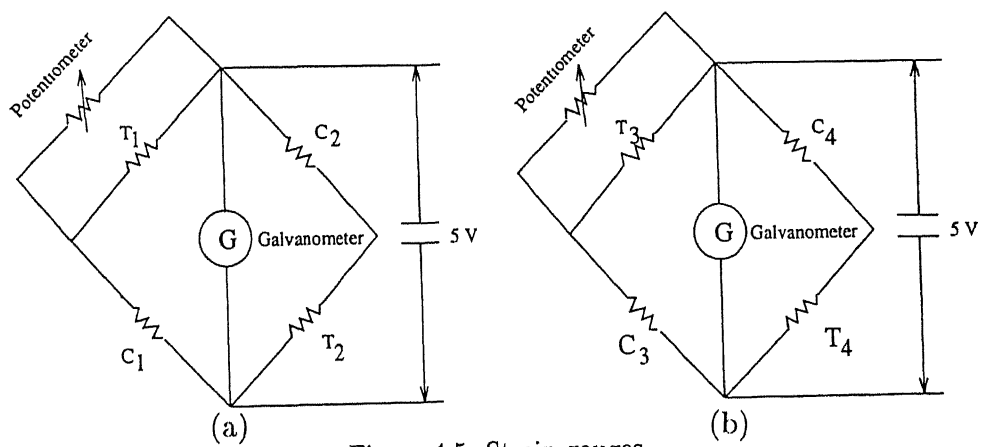


Figure 4.5: Strain gauges

4.2.2 Amplifier

As the output voltage available after the dynamometer is in terms of only a few millivolts a pre-amplification circuit is required before using the signal. The pre-amplification circuit has been designed and fabricated using a special purpose operational amplifier. The circuit is shown in the Fig. 4.6.

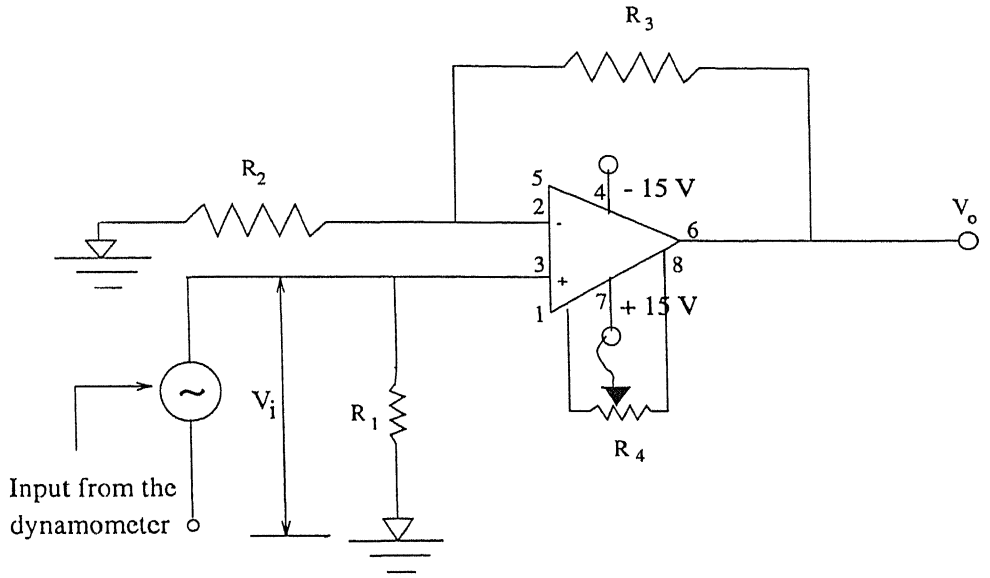


Figure 4.6: Amplification circuit

An operational amplifier amplifies the difference in the voltage signals at the two inputs, and can operate either in inverting or non-inverting mode. The voltage developed in the wheatstone bridge is fed as one input across the resistance R_1 to the op-amp, the other input is grounded with another resistor, R_2 ; R_3 being the feedback resistor. Required factor of gain is obtained by using appropriate values of the two resistors, R_3 and R_2 . Initially with the two inputs of the op-amp shorted and grounded, the output voltage is set to zero using the variable resistor, R_4 . This is called the input offset voltage correction. This is to be done carefully before using the circuit otherwise the op-amp will be driven into a saturation region giving a constant output voltage for any input signal. The gain used in the present work is

calculated as follows :

$$G = (1 + \frac{R_3}{R_2}) \quad (4.1)$$

The output voltage is found as

$$V_o = V_i G \quad (4.2)$$

where V_i is the input voltage to the amplifier as shown in the Fig. 4.6, which is the voltage across the galvanometer in the sensor circuit, Wheatstone bridge.

4.3 Analog to Digital Conversion

The signal from the amplification circuit is to be converted into digital form before feeding it to the software. Of the various techniques available for A/D conversion, Successive Approximation Method is the most popular method [23]. In this, technique, various output codes are fed into a D/A converter and the result is compared with the analog input via a comparator, as shown in Fig. 4.7. The way it is usually done is to set all bits initially to zero, and beginning with the most significant bit, each bit in turn is set to one. If the D/A output does not exceed the analog input signal voltage, the bit is left as a one, otherwise it is set back to zero. For an $n - bit A/D$, n such steps are required.

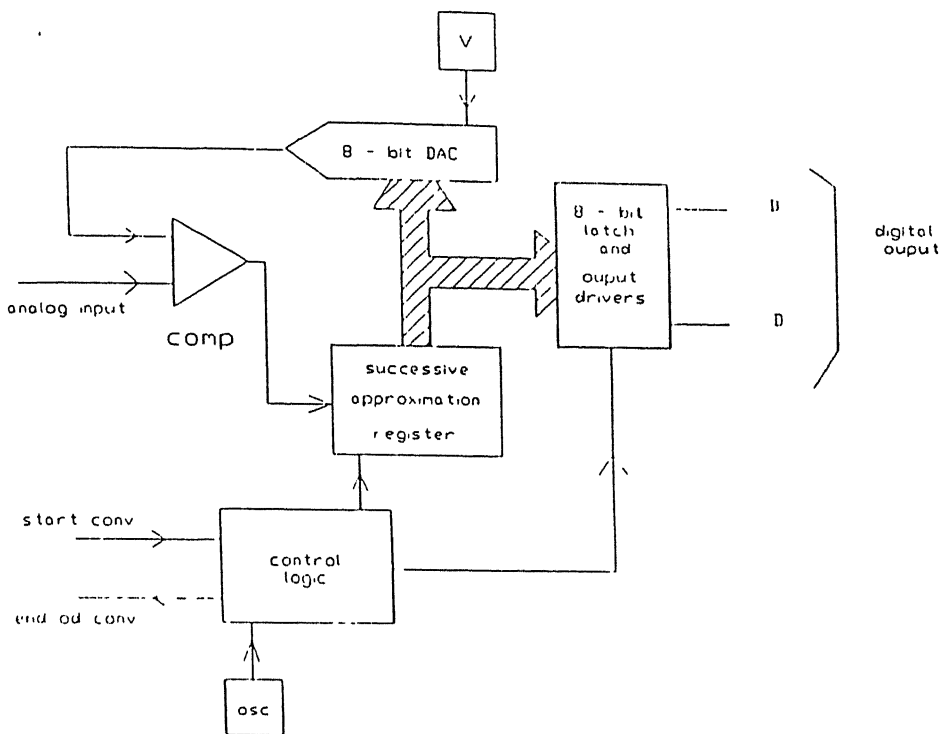


Figure 4.7: Successive approximation ADC, [26]

A successive approximation A/D module has a *BEGIN OF CONVERSION* input and *END OF CONVERSION* output. The digital output is always provided in the parallel format. Successive approximation A/D converters are relatively accurate and fast, requiring only ' n ' settling times of the DAC for n - bit precision. This type of converter operates on a brief sample of the input voltage and if the input voltage is changing during the conversion, the error is not greater than the change during that time.

A commercially available data acquisition card for *IBMPC/XT/AT* computers, *PCL-812* from Dynalog Microsystems Ltd., is used in the present work. This uses an industrial standard 12 - bit successive approximation converter *ADC574* to convert the analog inputs. The specifications and features of this card are shown in Appendix.

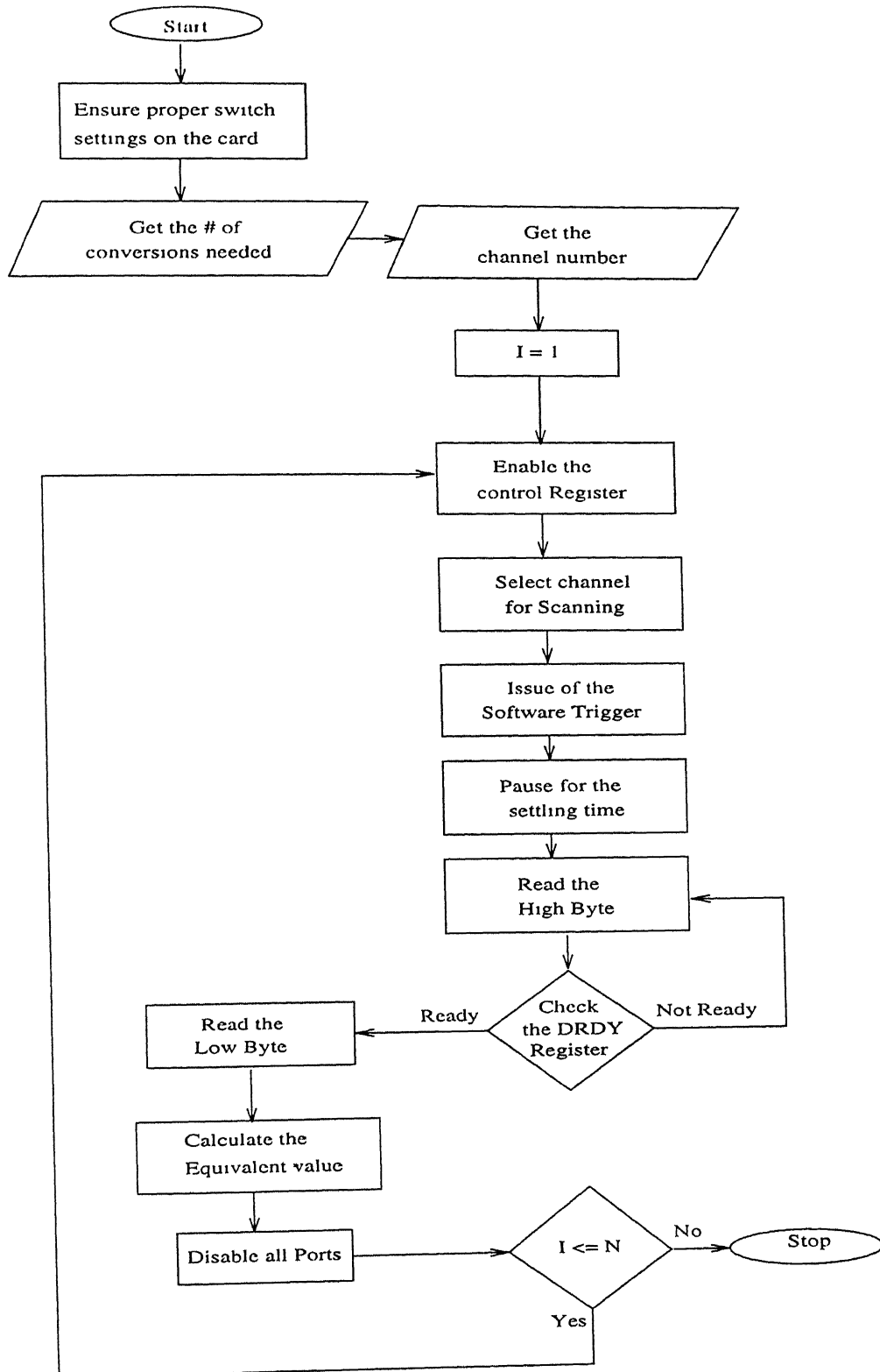


Figure 4.8: Flowchart for analog-to-digital conversion

The A/D conversion is triggered using a software, controlled by the application program issued software command. The data transfer is also performed using the program control. After the A/D converter has been triggered, the application program checks the *END OF CONVERSION* (EOC) bit of the A/D status register. If the EOC is detected, the converted data are transferred from the A/D data register to computer memory by the application program control. Fig. 4.8 shows the algorithm used for the writing the application for the A/D conversion.

4.4 Experimental Procedure

A software using "C" language has been developed as a part of implementation of the model. The program can run on any PC with "turbo C" compiler. The inputs to the program include cutting parameters (cutting speed, feed, depth of cut), tool geometry (back rake and clearance angles), work and tool materials, various machining costs and wear land criterion h_f^* . Wear coefficient, diffusion coefficient, and hardness of work-piece are read from the data files. The output of the program can be the optimum cutting speed for minimum cost or maximum production rate criterion, depending on the option selected. *Gilbert's model of economics of cutting has been used for evaluating optimum cutting conditions.* Fig. 4.9 shows the algorithm used for writing the application program.

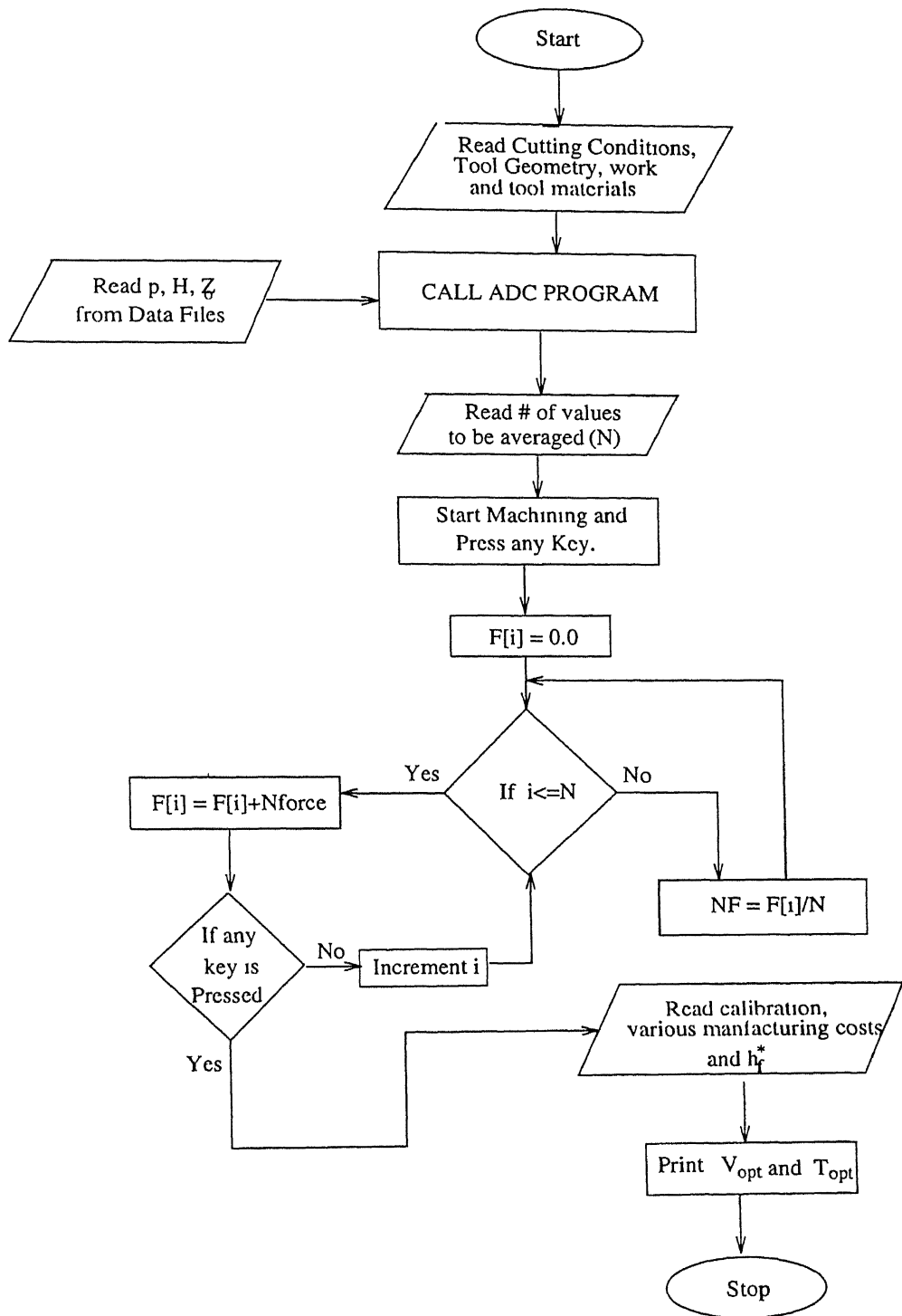


Figure 4.9: Algorithm for the Application program

Chapter 5

RESULTS and DISCUSSION

5.1 Machining of Steel with HSS

For evaluating optimal cutting conditions tool-life equation is to be well defined. Experiments were conducted for evaluating Taylor's tool life exponent ' n ' and constant ' C ' for HSS tool and Steel workpiece. Initial experiments were conducted with mildsteel workpiece and HSS with 10% Cobalt tool. Since mild steel is a ductile material there is a tendency of forming built-up-edge, and so the tool wear was not clearly visible with travelling microscope. Experiments were also conducted with high carbon steel workpiece and the same tool. In this case even at low cutting speeds the wear was rapid. Hence a medium carbon steel of grade *EN24* has been selected as the workpiece material.

In case of machining steel workpiece with HSS tool, it has been found that carbon from the tool diffuses into the workpiece even at low temperatures [23]. HSS tool has martensite matrix. In martensite matrix, layer of iron atoms are restrained from slipping over one another by dispersion of small carbon atoms. The interstitial carbon atoms start moving at temperature around $200^{\circ}C$. Figure 5.1 shows the variation of diffusion co-efficient of carbon with respect to 0.3% carbon steels with

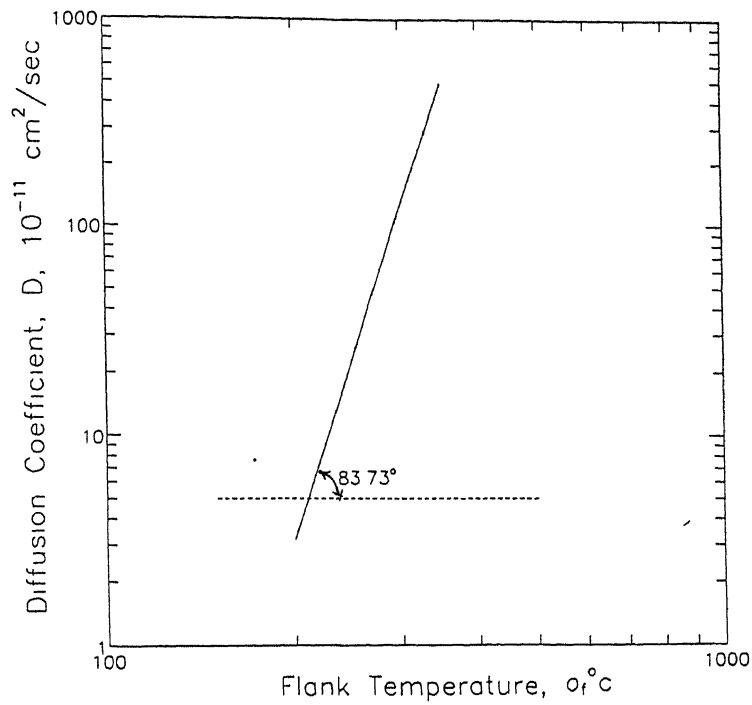


Figure 5.1: Variation of diffusion coefficient of carbon with respect to 0.3% C steel
(as in Eq. 3.4)

flank temperature [27] The value of p_λ is obtained from the figure.

5.2 Validation of the Model

Experiments were conducted at two cutting speeds, 56 and 72m/min. Both the experiments were conducted at the feed, 0.113mm/rev; depth of cut, 0.5mm; tool geometry, 0 - 10 - 6 - 6 - 10 - 0 - 0mm. At cutting speed 56m/min normal force was recorded with respect to time, t , taken in steps of 2min. Similarly, at 72m/min the normal force was recorded at time, t , taken in steps of 0.5min. The flank wear land was measured using a travelling microscope, normal force, N with a strain gauge dynamometer and time, t , with a stop watch. The recorded values are presented in Table 5.1 and Table 5.2.

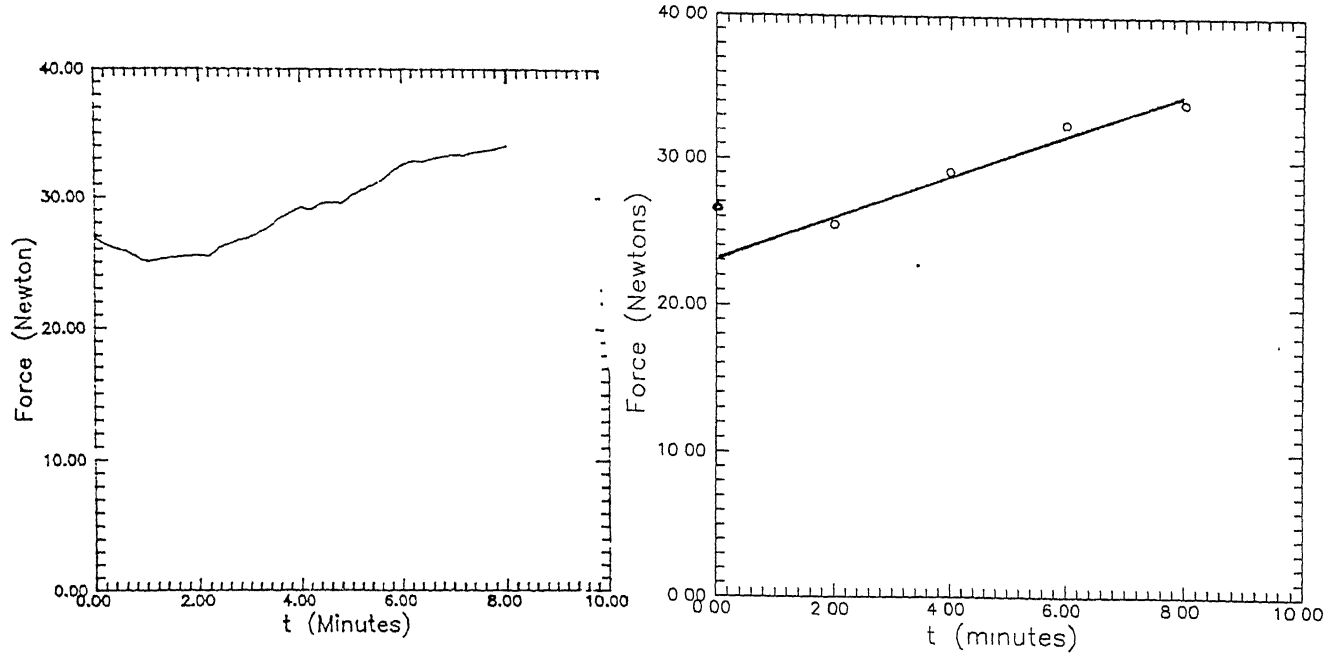
The normal force signal from the dynamometer was recorded using a plotter. Fig.5.2a shows the force signal recorded at cutting speed, 56 m/min with respect to time t and Fig. 5.2b shows the same plot with a best-fit line. Fig.5.3a shows the

Table 5.1: Experimental values at 56m/min

Time, t (min)	Normal Force, N (Newton)	Flank Wear land, h_f (mm)
0	26.85	0.0
2	25.5	0.09
4	29.2	0.18
6	32.5	0.32
8	34.0	0.40

Table 5.2: Experimental values at 72m/min

Time, t (min)	Normal Force, N (Newton)	Flank Wear land, h_f (mm)
0	21.4	0.0
0.5	20.9	0.09
1.0	22.9	0.16
1.5	25.0	0.23
2.0	27.0	3.4
2.5	28.7	4.1



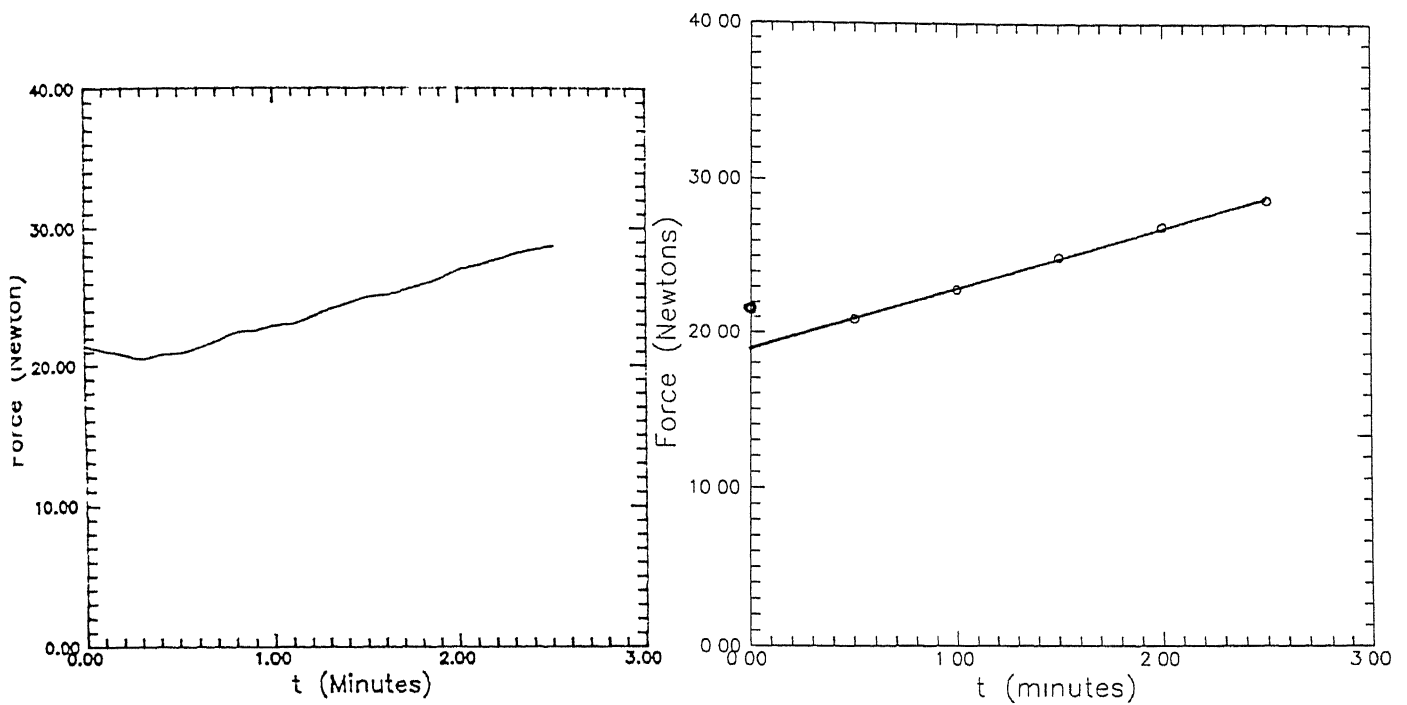
(a) Signal from dynamometer (b) Plot with best-fit

Figure 5.2: Variation of normal force with time at cutting speed, $56m/min$

force signal recorded at cutting speed, $72m/min$ and Fig. 5.3b shows the same plot with a best-fit line. It was found from the experiments that the normal force value dropped in the first few minutes of machining and then increased. This behaviour may be due to blunting of the sharp tool after a few minutes of machining, which is known as "initial break-in" phenomenon

Fig. 5.4 shows the variation of normal force, N with flank wear land, h_f for cutting speeds, 56 and $72m/min$. The linear increase of normal force with flank wear land is observed by previous investigators. As flank wear land grows, the rubbing action between the tool and workpiece increases, and hence the normal force increases.

Fig 5.5 shows the variation of flank wear land with time for the two specified speeds. Taking h_f^* (flank wear land criterion) as $0.4mm$ Fig. 5.6 has been plotted with cutting speed, V_c against Tool life, T in logarithmic scale. In Fig. 5.6 the continuous line is the experimental result. From the experimental line the values of



(a) Signal from dynamometer

(b) Plot with best-fit

Figure 5: Variation of normal force with flank wear and cutting speed

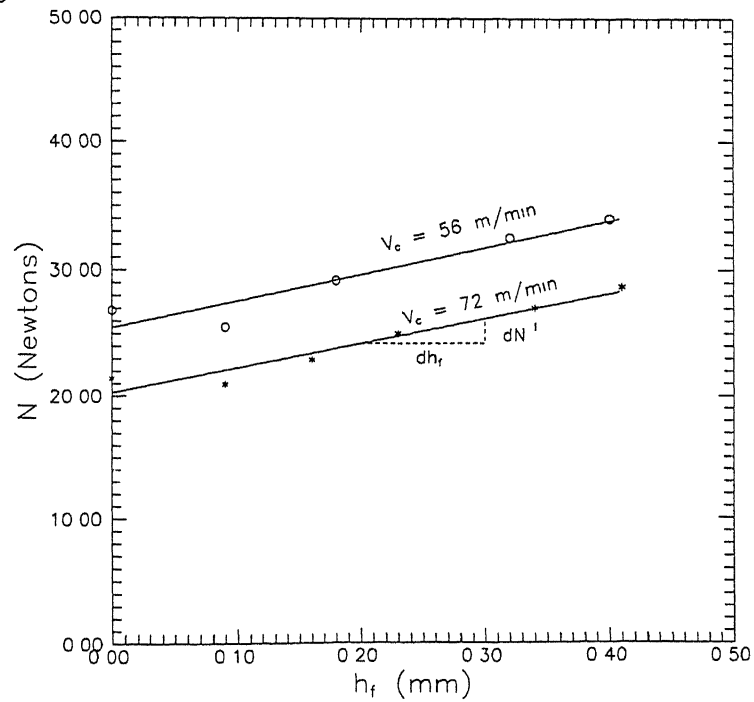


Figure 5.4: Variation of normal force with flank wear and cutting speed

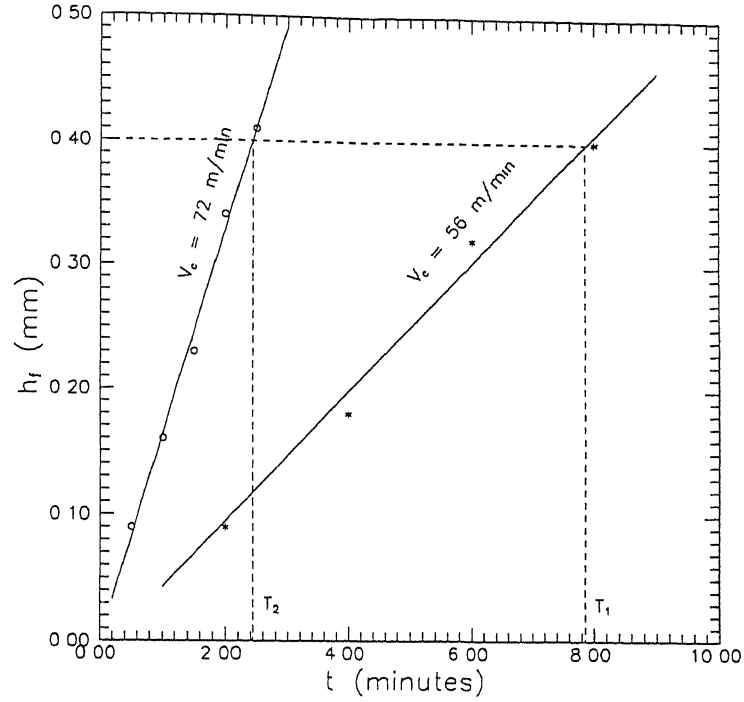


Figure 5.5: Variation of flank wear land with time

the exponent n and constant C are found out to be 0.18 and 81 respectively.

The value of $A(\frac{dN_f}{h_f})$ can be calculated from Fig. 5.4. Substituting the cutting conditions, tool angles, $p, A, Z_o, h_f^* = 0.4 \text{ mm}$ and H in the model developed in Chapter 3 we get exponent n as 0.21 and constant C as 88. In Fig. 5.6 the broken line is the result obtained using the model.

Using the application program developed, the optimum cutting speed was found out. Using the values of n and C , values obtained from the model, $\lambda_1 = \text{Rs } 5.25$, $\lambda_4 = \text{Rs } 87.50$, and $t_{ct} = 2 \text{ min}$ in Eq. 2.4 the optimum cutting speed for minimum cost was obtained as 36.4 m/min . Using the above values in Eq. 2.5 optimum cutting speed for maximum production rate was obtained as 73.35 m/min .

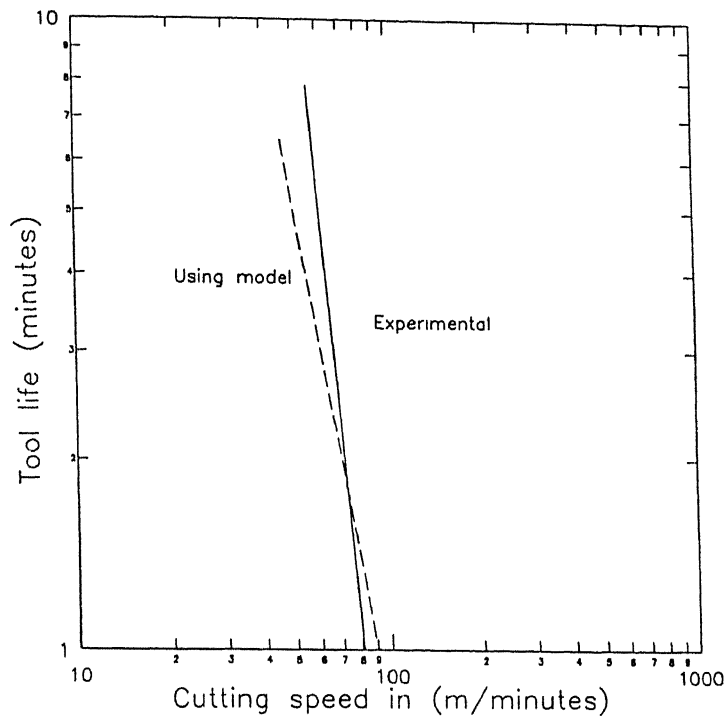


Figure 5.6: Cutting speed V vs Tool life

5.3 Discussion

There is discrepancy in the experimentally calculated values (Eq. 4.1) of ' n ', ' C ' and those obtained by using the model (Eq. 3.20). The value of ' p ' used in the model was based on the diffusion of carbon in 0.3% carbon steel. But the work material used is *EN24* which has a composition of 0.35%-0.4% carbon. Cobalt is good decarburiser. The presence of 10% cobalt in the tool affects the diffusion coefficient. If the diffusion coefficient for the material combination used in conducting the experiments is known a better result can be expected.

Chapter 6

CONCLUDING REMARKS

An Adaptive Control System for on-line evaluation of optimal cutting conditions with minimum experiments had been attempted. Adhesive wear was assumed as predominant wear mechanism. The model developed is not sensitive to feed and depth of cut variations. Understanding of diffusion mechanism is very important. If the diffusion co-efficient values is better known, accurate results can be expected. The model is very useful in industries wherein the tool, work materials change frequently, and optimal cutting conditions have to be evaluated each time they change. A database with diffusion co-efficients and material properties will be useful for industrial implementation. The application program developed by the author can be updated with more versatile optimization techniques for better results.

6.1 Scope for future work

Some of the prospective areas which are related to the present work are:

- A model sensitive to variation of feed, depth of cut may be attempted (*increase in the number of parameters will complicate the model*)

- The diffusion coefficient is critical parameter. By understanding the diffusion mechanism for different tool-work combinations a more complete Adaptive Control System (*ACS*) can be developed.
- Analysis has been carried out only for steel work-pieces and HSS, carbide tools. Analysis can be done for other tool-work combinations also.
- The application program can be updated with more versatile optimisation techniques for better results.
- A CCD camera, which can measure the flank wear land on-line, can be included for better results.
- A closed loop *ACS* may also be attempted.

REFERENCES

- [1] Archard, J.F., "Constact and Rubbing of Flat Surfaces," *Journal of Applied Physics*, Vol.24, No.3, 1953.
- [2] Rubenstein, C., "An Analysis of Tool Life Based on Flank-Face Wear, Part 1: Theory," *Journal of Engineering for Industry, Trans. ASME*, Feb. 1976, pp.221-226.
- [3] Ghosh, A. and Mallik, A.I., Manufacturing Science, Affiliated East-West Press Pvt. Ltd., 1993.
- [4] Armarego, E.J.A. and Brown, R.H., The Machining of Metals, Prentice-Hall, Englewood Cliffs, New Jersey, 1969.
- [5] Gomayel, J.I.El., and Bregger, K.D., "On-Line Tool Wear Sensing for Turning Operations," *ournal of Engineering for Industry, Trans. ASME* Feb. 1986, pp.44-47.
- [6] Davies, R., "A Tentative Model for Mechanical Wear Process," Symposium on Friction and Wear, Detroit, 1957.
- [7] Dawihl, W., "Influence of Diffusion and Alloy Formation on Resistance to Wear of Carbides Compositions," *Zeitschrift Technische Physik*, Vol.21, 1958.
- [8] Trent, E.M., Metal Cutting, Butterworths, London, 1984.

- [9] Loladze, T. N., "Wear of Cutting Tools," Mashiz, Moscow, 1951, and "Adhesion and Diffusion Wear in Metal Cutting," *Journal of Institute of Engineers*, Vol.XLIII, No.3, Nov., 1962.
- [10] Ghosh. A., "Wear of Cutting Tools," PhD Thesis, University of calcutta, 1967.
- [11] DeVor, R.E., Anderson, D.L., Zdeblick, W.J., "Tool Life Variation and Its Influence on the development of Tool Life Models," *Journal of Engineering for Industry, Trans. ASME*, Aug. 1977, pp.578-584.
- [12] Akgerman, N., Frisch, J., "The Use of Cutting Force Spectrum for Tool Wear compensation during Turning," *Proc. 12th Int. Machine Tool Design and Research Conf.*, 1991, pp.517-526.
- [13] Rossetto, S., and Zompi, A., "A Stochastic Tool-Life model," *Journal of Engineering for Industry, Trans. ASME*, Vol.103, Feb. 1981, pp.126-130.
- [14] Koren, Y., Ulsoy, A.G., Danai, K., "Tool Wear and Breakage Detection Using a Process Model," *Annals of CIRP*, Vol.35/1, 1986, pp.283-288.
- [15] Rao, S.B., "Tool Wear Monitoring Through the Dynamics of Stable Turning," *Journal of Engineering for Industry, Trans. ASME*, Vol.108, Aug. 1986, pp.183-190.
- [16] Danai, K., and Ulsoy, A.G., "A Dynamic State Model for On-Line Tool Wear Estimation in Turning," *Journal of Engineering for Industry, Trans. ASME*, Vol.109, 1987, pp.396-399.
- [17] Oraby, S.E., and Hayhurst, D.R., "Development of Models for Tool Wear Force Relationships in Metal Cutting," *Int. J. Mech. Sci.*, Vol.33, 1991, No.2, pp.125-138.

- [18] Kaye, J.E., Yan, D.H., Popplewell, N., and Balakrishnan, S., "Predicting Tool Flank Wear Using Spindle Speed Change," *Int. J. Mach. Tools Manufact.*, Vol.35, No.9, 1995, pp.1309-1320.
- [19] Gilbert, W.W., *Machining Theory and Practice*, p.465, ASME, Metals Park, Cleveland, OH, 1950.
- [20] Martin, P., Richard, J., and Veron, M., "The Influence of Cutting Speed Variations on Tool Wear for Optimal Control Machining," *Annals of CIRP*, Vol.28/1, 1979, pp.7-11.
- [21] Micheletti, G.F., Deflippi, A., and Ippolito, R., "Tool wear and Cutting Forces in Steel Turning,," *The Proceedings of the CIRP - ASTM Conference*, Ann Arbor, Mich., Sept., 1967.
- [22] Moriwaki, T., "Sensing and Prediction of Cutting Tool Failure," *Bull. Japan Soc. of Prec. Engg.*, Vol.18, N0.2, June 1984, pp.90-96.
- [23] Cook, N.H., *Manufacturing Analysis*, Addison Wesley, 1966.
- [24] Shaw, M.C., *Metal Cutting Principles*, BPB Publications, 1987.
- [25] Battacharya, A., Ghosh, A., Ham, I., "Analysis of Tool Wear Part II: Applications of Flank Wear Models," *Journal of Engineering for Industry, Trans. ASME*, Feb. 1970, pp.109-114
- [26] P.Horwitz and W.Hill, *The art of electronics*, Cambridge Univirsity Press (1992).
- [27] Smithells, *Metals Reference Handbook*, American Society for Metals (1984).

APPENDIX

- Workpiece material : *EN24 steel*
- Workpiece composition: *0.35 - 0.45% C;*
0.45 - 0.6% Mn;
1.3 - 1.8% Ni;
0.9 - 1.4% Co;
0.2 - 0.3% Cr;
0.1 - 0.35% Si;
rest is iron.
- Workpiece hardness : *260 BHN*
- Cutting tool material : *HSS with high cobalt*
- Cutting tool composition *18% W, 4% Cr, 2% V, 10% Co*
- Tool geometry : *0 - 10 - 6 - 6 - 10 - 0 - 0mm*
- Specification of lathe : *Type : LB17*
center height : 170 mm
center distance : 1000 mm
swing over bed : 350 mm
swing over cross slide : 170 mm
spindle speeds : 45 - 2000 rpm
feeds : 0.005 - 1.4 mm/rev.

•Specification of A/D card Model : PCL 812

- : 16 single analog input channels
- : 12 bit successive approximation ADC
- : switch selectable bipolar input ranges as $\pm 1V$, $\pm 2V$, $\pm 5V$, $\pm 10V$
- : trigger modes by software command, programmable pacer or external pulse trigger
- : data transfer by program control, interrupt handler routine or direct memory access.

•Specification of Op-amp Make : PMI

Type : 45 - 2000 *rpm*

Power supply : voltage $\Delta V = 30$

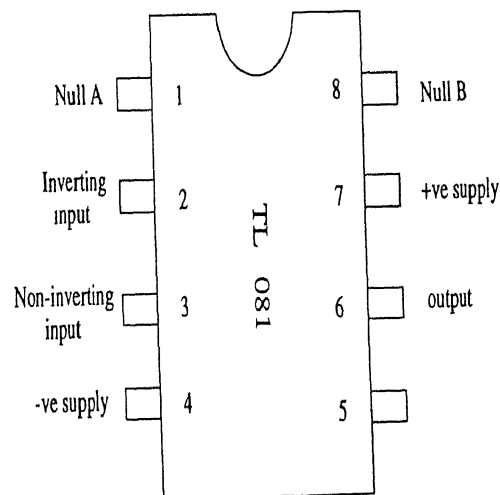
Maximum Voltage drift : $10 \mu V/^{\circ}C$

Maximum Voltage offset : $7.5 mV$

Maximum current offset : $1 nA$

Maximum current bias : $6 nA$

Pin Diagram:



•Typical Wear Coefficients [24]

Materials	Wear Coefficient, $Z \times 10^{-3}$
Mild steel on hard steel	0.01
Hard steel on mild steel	0.002
Tungsten Carbide on Tungsten Carbide	1×10^{-6}
Hard steel on Hard steel	1.3×10^{-4}
Tungsten Carbide on mild steel	4×10^{-6}
Copper on mild steel	1.5
Stainless steel on Stainless steel	21

- Variation of diffusion coefficient of $WC \rightarrow Fe$
with respect to temperature, deg C.

